AN EXPERIMENTAL ANALYSIS OF HORIZONTAL HYDRO AUGER PROTOTYPE DESIGNS USED TO GENERATE POWER FROM WATER WITH A VELOCITY

A Thesis

Submitted to the Office of Graduate Studies

of Saint Martin's University

in Partial Fulfillment of Requirements

for the Degree of

Master of Mechanical Engineering

by

Jillian Diane Coday, B.S.M.E

_____

Paul E. Slaboch, Director

Graduate Program in Mechanical Engineering

Lacey, Washington

August 8, 2016

AN EXPERIMENTAL ANALYSIS OF HORIZONTAL HYDRO AUGER PROTOTYPE DESIGNS USED TO GENERATE POWER FROM WATER WITH A VELOCITY

Abstract

by

Jillian Diane Coday

The horizontal power generation application of the traditional Archimedean screw was investigated. The power generation theory for the specific application tested was researched and reviewed for efficiency and power calculations. The Horizontal Hydro Auger (HHA) prototypes were developed using Autodesk Inventor for the 3D modeling. All of the prototypes were 3D printed using a PolyJet process, corresponding equipment was manufactured, and a repeatable experiment process was created to obtain consistent results.

Nine individual tests were completed in total. The tests were broken up into Part 1 and Part 2 for two different water velocity scenarios. The tests involved controlled variables including two different pitch geometries, a PVC pipe feature, an edge feature added to the outer edge of the blade, and two different water depths with corresponding velocities. Each test ran until steady state was achieved and data collection was started at this point. The water velocity, prototype RPM, percentage of water covering prototype, volts, amps, and power generated was recorded for each test. The power generated in each test was analyzed using reference developed horizontal auger power theory. Efficiencies and total power generated were calculated and compared for each scenario, a design was chosen as the best performing prototype related to the experimental results, and suggestions for future research and development were discussed.

ACKNOWLEDGMENTS

I would like to thank my parents, Dan and Diane Hamilton, my grandfather, Joe Chainey, and my husband, Eric Coday, for their never ending support and encouragement.

A special thanks to Joe Lentz for assisting in the experiment set up, to Scott Hoffman and Mike Coles for 3D printing the prototypes, and to Joe Jasniewski for LabVIEW assistance.

I would also like to thank my advisor, Dr. Paul Slaboch, for his help and guidance through this process.

CONTENTS

FIGURES

TABLES

SYMBOLS

English

Δd	Change in Water Depth
A_b	Wet Blade Area
C_D	Drag Coefficient
C_P	Coefficient of Power
D	Archimedes Screw Outer Diameter
d_0	Inflow Water Depth
D_H	Archimedes Screw Hub Diameter
F_D	Force Exerted on Screw Blade
F_{hyd}	Hydrostatic Force
g	Gravitation Acceleration
h	Height of the Archimedes Screw from the Horizontal
L	Archimedean Screw Length
L_b	Length of the HHA
m	Number of Blades
P	Static Pressure
P_Δ	Hydrostatic Pressure Difference
P_0	Stagnation Pressure
P_{blade}	Blade Power
P_{Ex}	Experimental Power
P_{hyd}	Hydraulic Power
P_M	Mechanical Power
P_T	Potential Power Produced by HHA
P_{Th}	Theoretical Power of the Water Velocity
P_{Total}	Power of the Screw
R	Effective Radius
R_i	Hub Radius
R_o	Outer Blade Radius
T	Torque

v	Water Velocity
v_0	Entry Velocity
v_1	Approach Velocity
V_b	Blade Velocity
V_c	Stream Flow Velocity
V_r	Relative Velocity
Greek	
α	Position Angle of the Archimedes Screw
ρ	Water Density
ω	Angular Velocity
η_A	Actual HHA Efficiency
η_{hyd}	Hydraulic Efficiency

CHAPTER 1: Introduction

1.1 Background and Motivation

Electricity is a crucial element to everyday life and success for everyone all over the world. Without electricity, simple daily tasks become challenging, technology is extremely limited, access to health care and medicine is crude, and formal education is reduced to a bare minimum. People thrive in a world with electricity and those who do not have access to it are forced to live in an environment that does not allow them to be successful. The worlds dependence on fossil fuels has recently brought attention to green energy and how it could be sourced. With lots of research performed on large, expensive projects such as underwater turbines, wind turbines, and solar panels, not much attention has been given to smaller scale methods. Underwater hydropower collection in a smaller scale could bridge the gap between fossil fuels and traditional energy collection methods by producing a sustainable method that is easily accessible all over the world.

A characteristic of underwater energy collection that has been overlooked is the ability to be environmentally friendly in addition to being successful. Current underwater turbines have several negative effects to surrounding habitats whether it be anchoring lines into the sea floor, or fast moving blades that slice up the water and wildlife. Less expensive, environmentally friendly, smaller scale energy collection sources could mean that a rural town in a third world country could have access to technology without having to raise hundreds of thousands of dollars. These devices need to be developed and could be a benefit to areas that cannot afford the investment of the large scale energy collection systems.

The Horizontal Hydro Auger (HHA) represents a realistic method of energy collection that is relatively small in size, potentially low cost, and could eliminate harm to local wildlife. This experimental device uses similar principles to the hydraulic Archimedean screw. Historically, the Archimedean screw has been used to lift water from a low channel a higher field above to irrigate crops seen in Figure 1.

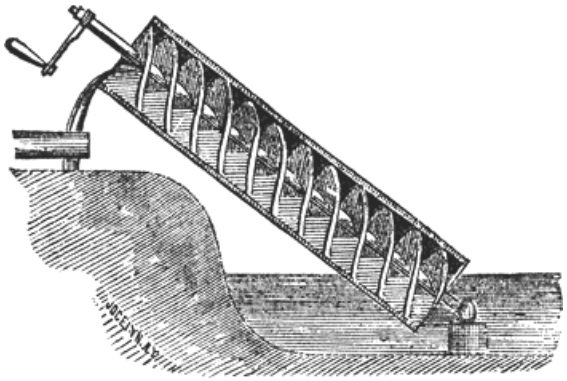

Figure 1: Traditional Archimedes Screw (1)

In the last century, the screw has been modified to run in reverse and is used all over the world as a generator taking advantage of the minimal head difference of small waterfalls and dams in an efficient inclined position. Applying the Archimedean screw theory to function in horizontal applications could be the answer for the small, inexpensive energy collection systems.

This thesis will study the development of the horizontal Archimedean screw application and analyze an experimental prototype. The goal of this thesis was to design several HHA prototypes, develop a repeatable experimental process to test the power generation capabilities of those prototypes, and provide a recommendation for future work to create an efficient and functional device to harness the kinetic energy of rivers, currents, and other moving bodies of water. The theory and process behind building the prototype will be discussed and experimental data that was collected will be presented and compared to determine the best option.

1.2 Literature Review

This thesis discusses the study and experimental process of validating a horizontally mounted hydro auger prototype used similarly to a reverse Archimedean screw. An investigation of the Archimedean screw used as a generator was necessary in order to understand screw geometry and basic efficiencies. Further research included finding similar cases to the horizontal hydro auger and comparing geometry, theory, and results.

1.2.1 Archimedean Screw Theory

Muller and Senior describe the general theory and basic conclusions about the screw being used as an energy converter. (1) Figure 2 shows a schematic of the inclined Archimedean screw and associated geometric values of interest where L, is the screw length, D, is the outer screw diameter, D_H, is the hub diameter, h, is the height of screw in reference to the horizontal, and, α, is the angle of the screw.

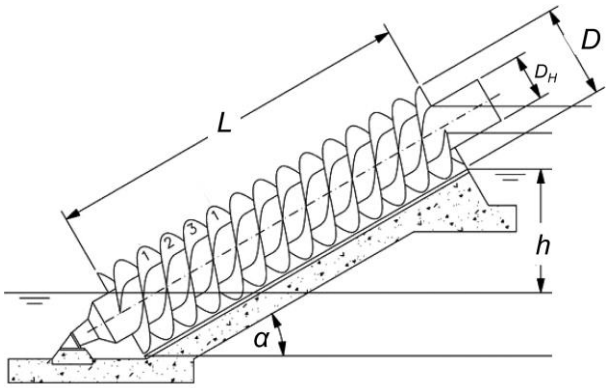

Figure 2: The Archimedean Screw shown with Labeled Geometry (1)

The theory behind the Archimedean screw used as a power converter has only recently been developed and analyzed. (1) In order to determine efficiencies, the screw's geometry is linked to its mechanical efficiency in a theoretical model and compared experimental results. The theoretical efficiency for the screw is found as

$$\eta_{th} = \frac{P_\Delta}{P_{hyd}} \quad (1)$$

where P_Δ is the hydrostatic pressure difference and P_{hyd} is the hydraulic power. This relationship between the hydraulic power and total power is determined from the hydrostatic pressure difference and the horizontal screw velocity. The forces on the screw from the pressure differences can be broken down into the hydrostatic forces due to geometry (1)

$$F_{hyd} = \frac{(d_0+\Delta d)^2 - d_0^2}{2} * \rho * g \quad (2)$$

where F_{hyd} is the hydrostatic force, d_0 is the inflow water depth, Δd is the change in water depth, ρ is the density of water, and g is the gravitational acceleration. (1) The hydrostatic pressure difference between up and down stream velocities acts on the blades and moves them with a velocity of v_1

$$v_1 = \frac{d_0}{d_0+\Delta d} * v_0 \quad (3)$$

where v_1 is the approach velocity and v_0 is the entry velocity. (1)

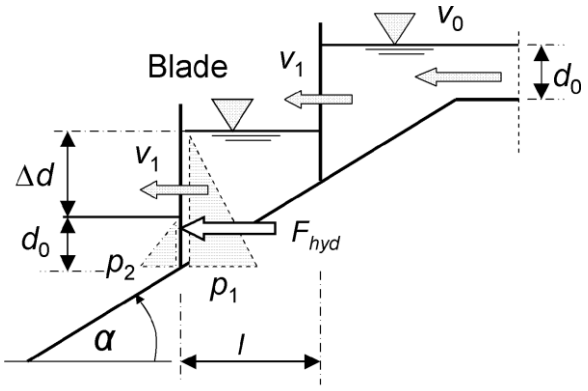

Figure 3: Forces Acting on Individual Screw Blades of the Archimedean Screw (1)

Individual screw blade power is hydraulic force times velocity of the fluid moving inside the screw as shown in Eq. 4. The forces acting on the screw blades are shown in Figure 3.

$$P_{blade} = F_{hyd} * v_1 \quad (4)$$

Multiplying the blade power, P_{blade}, by the number of blades, m, produces the total power, P_{Total}, of the screw

$$P_{Total} = m * P_{blade}. \quad (5)$$

The total power can now be found as

$$P_{hyd} = \rho * g * d_0 * v_0 * \Delta d * m \quad (6)$$

where P_{hyd} is the hydraulic power, ρ is the density of water, and g is the gravitational acceleration, v_0 is the entry velocity, d_0 is the inflow water depth, Δd is the change in water depth, and m is the number of blades. (1)

When the Archimedean screw is used in reverse as a generator Eqs. 1-6 can determine the power generated from the forces of the fluid acting on the screw. These equations are all relative to gravity which gives the water at the top of the screw the potential energy to ultimately turn the system.

The efficiency of the screw is not just dependent on losses, but also screw geometry. (1) The experimental data from Muller and Senior indicates that efficiency increases with a decreasing screw position angle, α, and increasing number of turns on the screw itself. This also implies that for steeper angles a higher number of turns is desirable. (1) The experiment also showed that to maintain high efficiencies, the upstream water level should be kept constant and high compared to the radius of the screw. The most important conclusion is that screw efficiency increases with a decrease in head drop between turns and with an increasing ratio of inflow depth and screw radius. (1) The analysis of the screw used as a generator positioned at a traditional angle to the horizontal promotes additional research of the screw positioned parallel to the horizontal. This thesis will do this by exploring experimental results of the HHA prototype.

1.2.2 Current Innovative Products

Mounting the Archimedean screw horizontally is a new experimental technique that several researchers are developing for efficient energy collection. (1-4, 8-9) Similar to the systems described in the previous section, the horizontal axis rotor is required to utilize the kinetic energy of the flowing mass in which it is placed. The difference is the near zero mounting angle. The horizontal orientation forces the rotation of each screw blade and the screw rotations can generate electricity. (2) These HHA systems can be hooked up to a simple generator in order to transform the energy into usable electricity. Several different orientations have been experimentally investigated and installed in Europe. A power plant in Germany, shown in Figure 4, is an excellent example of using Archimedean hydropower by operating a 2.8m high screw that rotates at 28 RPM. (2) This low head system provides the city of Munich with a yearly energy production of about 400,000 KWh. (2)

Figure 4: The Hydroelectric Power Plant "Stadtbachstufe" in Munich (2)

These inventive solutions for energy conversion are very successful when there is small to minimal head difference. Completely horizontal applications, such as the example shown in Figure 5, have yet to be implemented in power plants, but create opportunities in canals, rivers, tidal currents, and other zero head situations. (2)

Figure 5: Photorealistic Representations of a Floating HHA in a Canal (2)

Recently, a remarkable prototype was developed by an industrial engineer from Florida. The Eco-Auger is a micro hydrokinetic energy converter which incorporates a tapered, double helical, flanged auger. (3) The device is mounted normal to water flow, smaller in size and more affordable than previous underwater turbines, and the creative design is fish friendly. Inventor W. Scott Anderson, shown in Figure 6, developed the devices to operate completely submerged in relatively shallow rivers with minimal impact on the environment. (3) This product is unlike any other Archimedean screw because of its completely horizontal operating characteristic. This device needs water depth of ten feet to operate and has proven in tests to capture 14 percent of the water's energy. (3) The model tested was a two-foot diameter prototype and according to Anderson, the amount of energy captured will increase as the diameter of the auger increases. (3)

Figure 6: Anderson with the Eco-Auger Prototype (3)

The Eco-Auger is a real world application of the HHA that could potentially change the hydropower industry. This thesis will explore some of the design aspects of the Eco-Auger.

1.2.3 Horizontal Archimedean Screw Theory

In order to attempt to understand the power generation ability of the HHA, some simplifications to the geometry and theory had to be made. Following the analysis of a similar experiment, the HHA will be based on the drag principle using the classical undershot waterwheel with flat blades. (4) The flat blades of the water wheel mimic the HHA surface normal to the flow. From this simplification, a flat blade perpendicular to flow can be the geometry used to calculate forces.

From basic fluid dynamic analysis, any object moving through a fluid will experience drag – a net force in the direction of flow due to the pressure or shear forces on the surface of the object. (5) To simplify forces on the HHA blades a waterwheel simplification is used and is shown in Figure 7 where R is an effective radius, A_b is the wet blade area, ω is the angular velocity rotating in V_c, the stream flow velocity. (4)

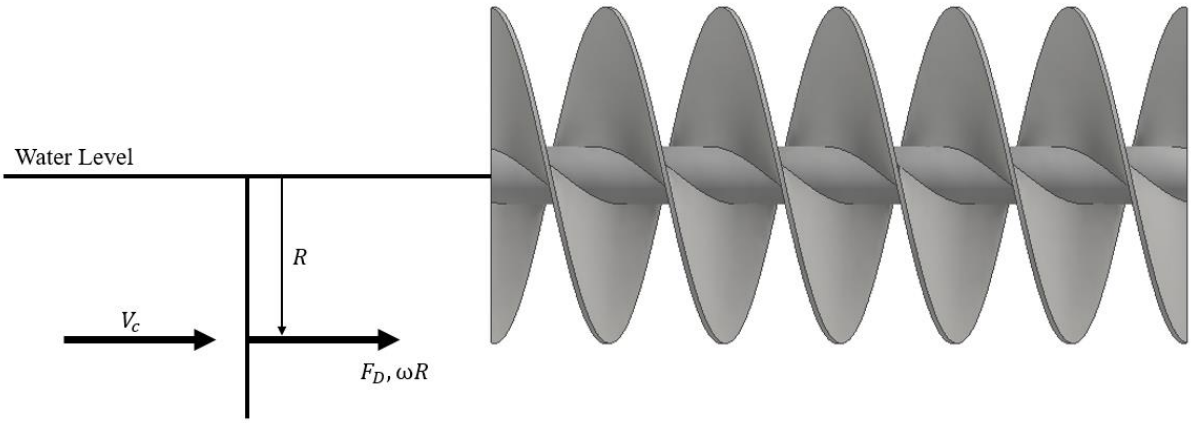

Figure 7: HHA Simplified as a Waterwheel Rotating in Flow (4)

The force exerted on one flat plate, simulating the flat screw blade is calculated by

$$F_D = \frac{1}{2} * \rho * V_r^2 * A_b * C_D \quad (7)$$

where ρ is the fluid density and C_D is the drag coefficient. (4) The relative velocity, V_r, is calculated using the difference between water velocity, V_c, and blade velocity, V_b

$$V_r = (V_c - V_b) \quad (8)$$

with the blade velocity calculated using

$$V_b = \omega * R \quad (9)$$

where ω is the angular velocity and R is the effective radius. (4) The effective radius, R, is calculated taking into account the actual outer blade radius minus the hub radius,

$$R = (R_o - R_i). \quad (10)$$

The wet blade area, A_b, is calculated by

$$A_b = L_b * (R_o - R_i) \quad (11)$$

where L_b equal to the length of the HHA and R_o and R_i as the outer radius of the blade and the hub radius of the HHA. (4) The drag coefficient was assumed to be 1.6 based on the table shown in Figure 8. (5)

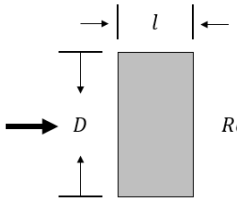

Rectangle

Reference Area
(b = length)
$A = b * D$

Coefficient of Drag

$$C_D = \frac{D}{\frac{1}{2} * \rho * V^2 * A}$$

l/D	C_D
≤ 0.1	1.9
0.5	2.5
0.65	2.9
1.0	2.2
2.0	1.6
3.0	1.3

Reynold's Number
$Re = 10^5$

Figure 8: Common Drag Coefficients for a Flat Plate (5)

For the waterwheel simplification with a flat blade of certain dimensions for l/D the coefficient of drag can be determined from the table in Figure 8. With the force acting on the blade, the potential power produced by the HHA can be calculated using the power equation

$$P_T = F_D * V_b. \tag{12}$$

Combining the power equation variables with the force equation to get the complete power equation

$$P_T = \frac{1}{2} * \rho * {V_r}^2 * A_b * C_D * V_b \tag{13}$$

where ρ is the density of water, V_r is the relative velocity, A_b is the wet blade area, C_D is the drag coefficient, and V_b is the blade velocity. (4) To break down the power equation it is expanded to show all variables

$$P_T = \frac{1}{2} * \rho * (V_c - V_b)^2 * A_b * C_D * \omega * R. \tag{14}$$

The potential power produced by the HHA can be calculated using Eq. 14. (4) The theoretical power produced by the velocity of the water can be calculated by using a blade tip speed ratio simplification. The blade tip speed ratio, γ, is the velocity at the tip, V_b, over the oncoming water velocity, V_c. (4) The blade tip speed ratio theory developed by Mayrhofer, Stergiopoulou, Pelikan, and Kalkani indicates a coefficient of power, C_P, that simplifies the theoretical power of the water velocity equation to be

$$P_{Th} = \frac{1}{2} * \rho * A_b * C_D * {V_c}^3 \tag{15}$$

where ρ is the density of water, A_b is the wet blade area, C_D is the drag coefficient, and V_c is the water velocity. (4) To be able to calculate the efficiency of the screw, the actual mechanical power of the screw is needed. The torque acting on the shaft is

$$T = F_D * R \tag{16}$$

where F_D is the force acting on the blade and R is the HHA radius. Taking the torque acting on the shaft, T, the angular velocity of the screw, ω, the mechanical power can be found according to

$$P_M = \omega * T. \tag{17}$$

With the theoretical power of the water velocity and mechanical power of the HHA calculated, the hydraulic efficiency of the HHA can be calculated by a simple ratio of the mechanical power, P_M, and the theoretical power of the water velocity, P_{Th}

$$\eta_{hyd} = \frac{P_M}{P_{Th}}. \tag{18}$$

This is the efficiency of the potential power generated by the HHA in comparison to the theoretical power generated by the water flow. The efficiency of the HHA prototype can be calculated using Eq. 19. This compares the potential calculated power of the HHA with the actual power test results

$$\eta_A = \frac{P_{Ex}}{P_T} \tag{19}$$

where P_{Ex} is the actual test results power measurement and P_T is the potential power produced by the HHA prototype. This efficiency calculation directly relates to the efficiency of the HHA prototype design. Eq. 18 shows the efficiency of the potential power of the HHA verses the power of the water velocity where Eq. 19 equates the efficiency of the actual tested HHA prototype. (4)

CHAPTER 2: Experimental Trials

2.1 Description of Experiment

The theory behind the HHA is still new in the hydropower world and not many experiments have been done to validate geometry or efficiency. In an attempt to discover optimal geometry and working conditions several experiments were conducted. The design, process, and set up will be discussed.

2.1.1 Auger Design

Four designs were modeled with slightly different features to test different auger geometry. Autodesk Inventor was the 3D modeling program used and the designs were 3D printed on a PolyJet Statasys Connex 500 printer in the VeroWhitePlus material. The material used mimicked high impact polystyrene and had a smooth surface finish. (6) The actual prototypes are solid plastic without honeycomb layers or uneven surfaces. The printer's precision characteristics printed the thin blades and edge features successfully. A PolyJet printer works similarly to a standard inkjet printer, but instead ink onto paper, layers of ultraviolet curable liquid photopolymer are layered onto a printing tray. (7) The support material was easily removed by scraping off the bulk of the material and then washing off the rest with a high pressure water wash. (7) The material was easily modified after printing to drill pin holes and file out the tight tolerance shaft through hole. The only down side to the material used was its relatively brittle characteristics and one prototype had to be reprinted due to a blade breaking.

The purpose of the experiment was to test different pitches to analyze the effect on the overall power output results and to examine the different pitches in two different velocities. The

addition of a PVC pipe attachment mounted on the outside the prototypes was another experimental design variable tested. The length, blade diameter, hub diameter and blade thickness of the prototype was chosen to be a constant throughout the process. These dimensions were limited due to the 3D printer's capacity and the water tunnel's width and depth at the testing facility. The prototype designs can be seen in Figure 9 through Figure 12.

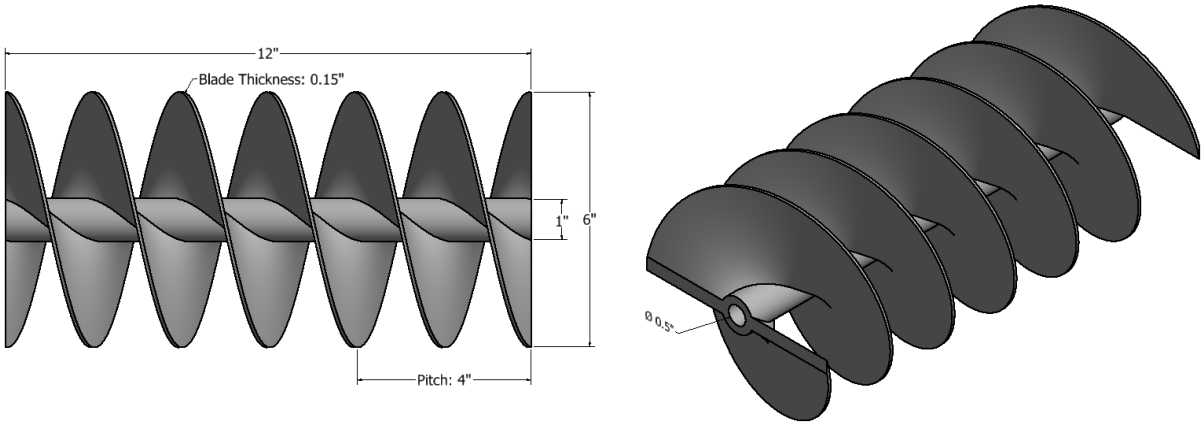

Figure 9: Auger 1

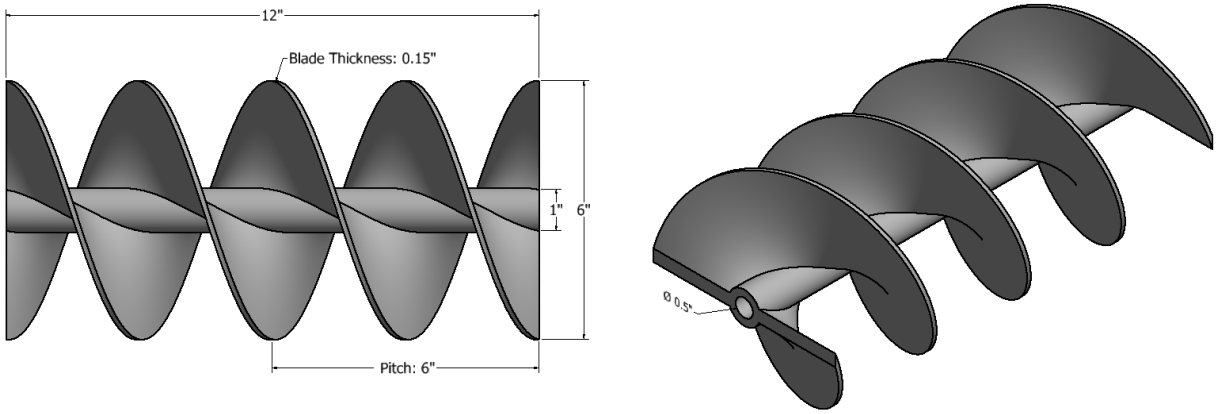

Figure 10: Auger 2

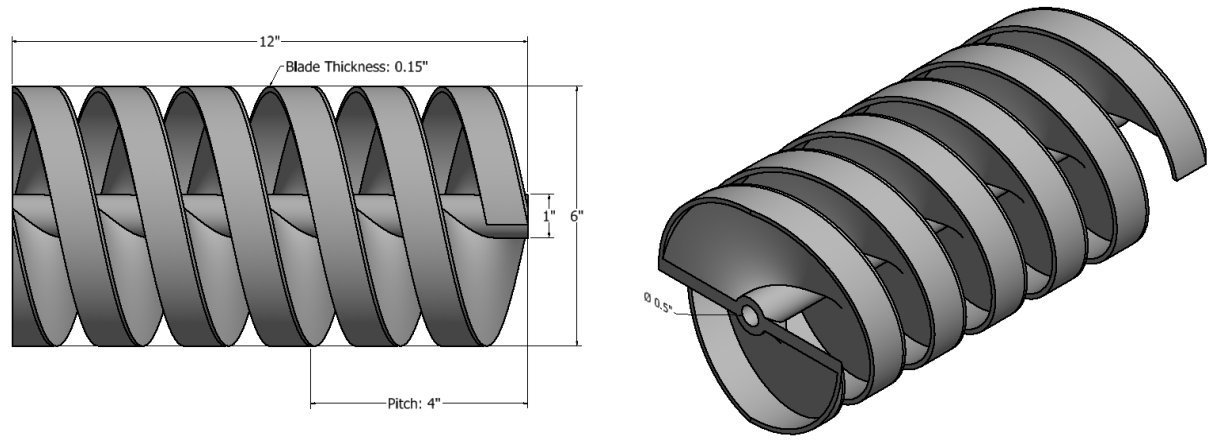

Figure 11: Auger 3

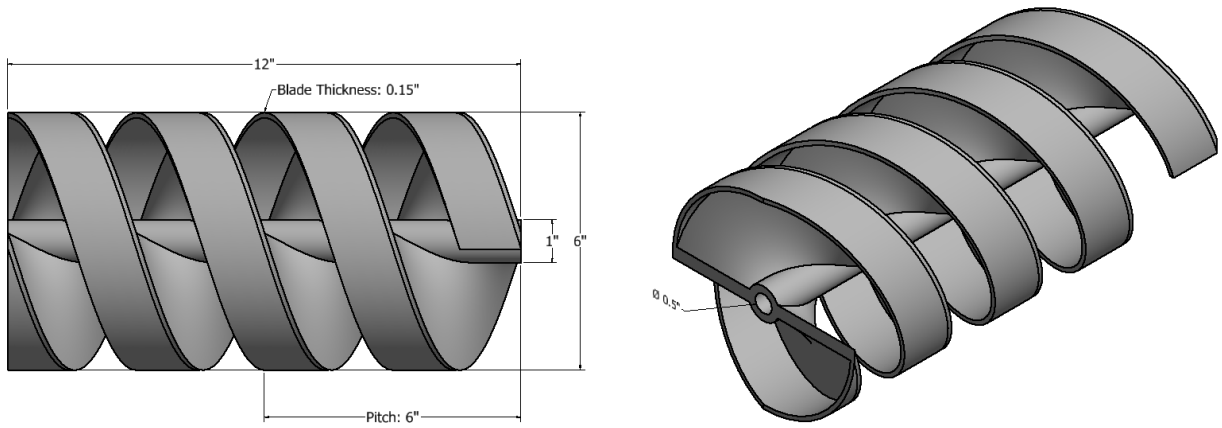

Figure 12: Auger 4

In addition to changing the pitch geometry an extra edge feature was added to the outer surface of the blade to create a bucket on the blade face. This design is seen in Figure 11 and Figure 12. There were two different auger pitches tested each with and without an edge feature. Table 1 shows a summary of all the prototype characteristics.

Table 1: Auger Descriptions

Design	Pitch (inches)	Blade Revolutions	Length (inches)	Hub Diameter (inches)	Blade Diameter (inches)	Blade Thickness (inches)	Edge Feature
Auger 1	4	3	12	1	6	0.15	N
Auger 2	6	2	12	1	6	0.15	N
Auger 3	4	3	12	1	6	0.15	Y
Auger 4	6	2	12	1	6	0.15	Y

2.1.2 Mounting Bracket

After the auger prototypes were designed the mounting bracket device, shown in Figure 13, was developed and manufactured. The bracket was necessary to hold the HHAs in the testing facility's water tunnel system. The water tunnel trough was approximately 18 inches tall by 12 inches wide and 15 feet long. The purpose of the mounting bracket was to create a constant, repeatable testing environment while having the ability to easily switch out auger prototypes. The mounting bracket requirements were determined from the definition of an HHA. The bracket must: hold the HHA horizontal, normal to the flow, as submerged as possible, and be the conversion between the kinetic energy of the water to electrical energy via generator.

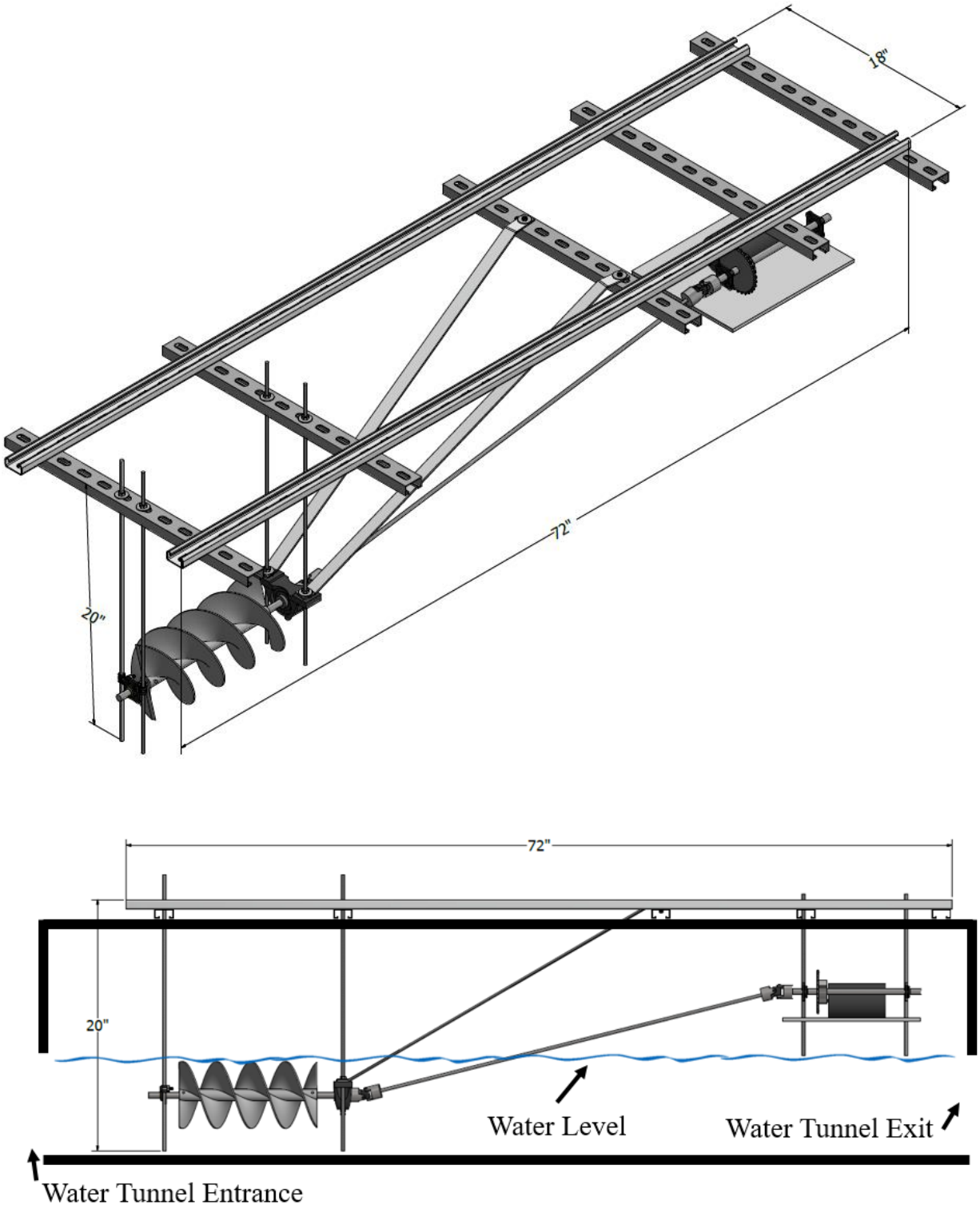

Figure 13: Mounting Bracket with Auger Prototype

With the requirements for the mounting bracket determined, construction was done using basic materials such as railing, steel bar stock, threaded rod, washers, nuts, bolts, and several bearings. The bracket structure was assembled by simple fasteners and spot welds. The auger prototypes were inserted onto a 14-inch main shaft which was fitted with bearings and alignment rods to secure it to the bracket structure, shown in Figure 14. In an attempt to minimize friction, the sealed bearing with grease inside was disassembled and soaked in a thinning agent. To secure the auger prototypes in place on the main shaft, holes were drilled through for cotter pins.

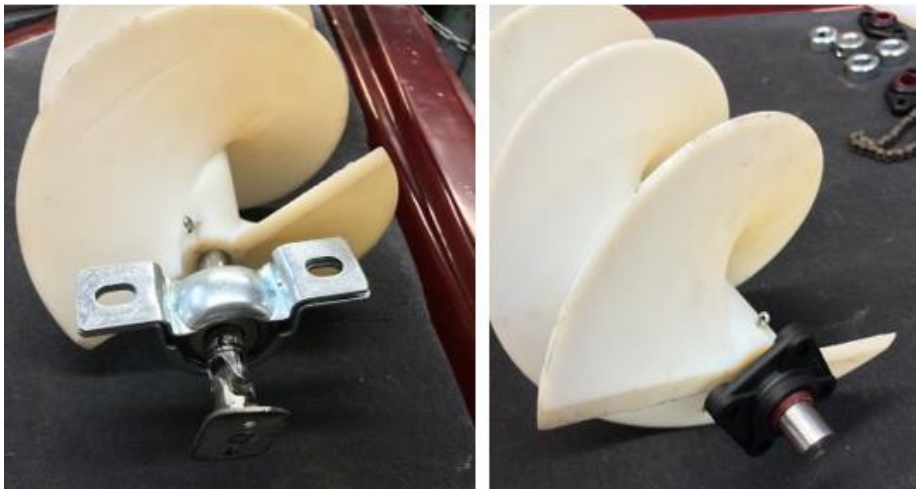

Figure 14: Auger Prototype on Main Shaft with Bearings

Another performance variable used was a 6-inch diameter PVC pipe to force water into the auger opening. This was attached to the threaded rod using bolts and washers, shown in Figure 15, and held the HHA along the main shaft. The PVC feature was only used for certain HHA prototypes and was easily removable. To transfer the rotational motion from the auger to the generator above water, the main shaft connected to the 3-foot-long drive shaft through a u-joint fastener, shown in Figure 16. Above the water the drive shaft connected to the 14-inch long gear shaft through another u-joint fastener. Both of the u-joint fasteners required a custom spot weld modification to assure no slippage when rotating underwater.

Figure 15: PVC Pipe Attached to Main Shaft

Figure 16: Drive Shaft Connected to Gear Shaft

The gear shaft was positioned horizontally on the 14-inch long base board for the generator. The base board that held the gear system was positioned underneath the main strut bracket and positioned at an angle. This created a straighter line for the drive shaft and reduced friction from the u-joint fasteners. The gear system used to connect the gear shaft to the generator consisted of: a 3.5-inch diameter gear with a set screw and 40 teeth, a 1-inch diameter gear with 11 teeth connected to the generator shaft, and a 1 ft long metal loop chain. To convert

the rotational energy into electricity a small 12-volt DC generator was mounted on the base board. The gear system and base board assembly can be seen in Figure 17.

Figure 17: Gear System on Base Board Assembly

One of the most important parts of the bracket was the bracing that kept the HHA in one place during water flow. The threaded rods shown in Figure 18 was used as bracing elements in several different places to ensure zero linear movement by the HHA. Using the threaded rod allowed for on the spot height adjustments that needed to be made at the time of testing.

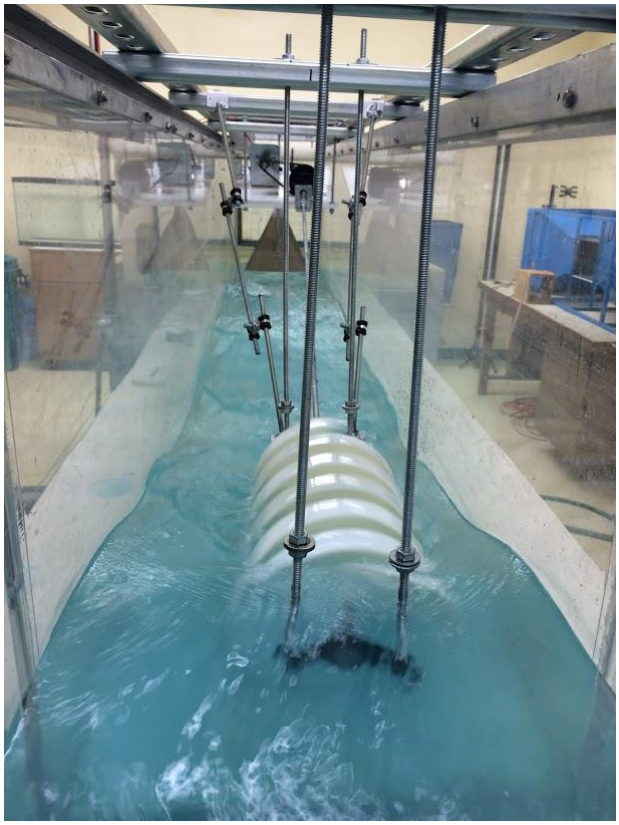

Figure 18: Threaded Rod Bracing

The final assembly for the mounting bracket is shown in Figure 19, the prototype shown in this picture is one with the PVC pipe addition. This mounting bracket system was custom built to fit in the water tunnel, allow for easy auger prototype interchangeability, and to convert the energy of the water to electricity.

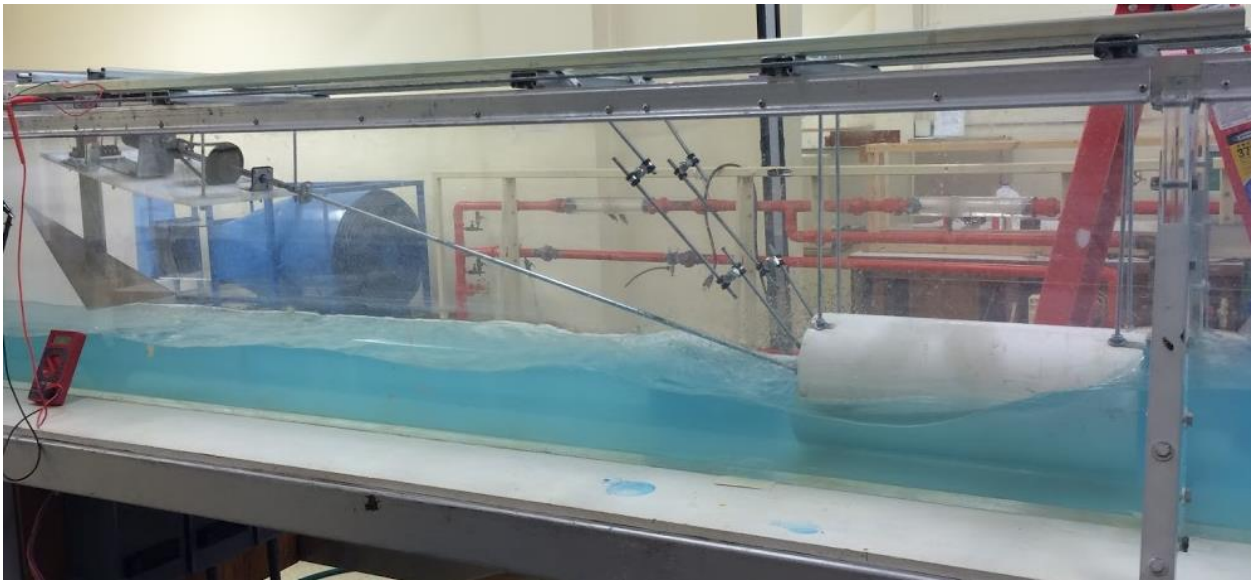

Figure 19: Final Mounting Bracket Assembly

2.1.3 Energy Collection and Instrumentation

To measure the power output of the screw LabVIEW software and a National Instruments MyRIO measurement device was used along with a Fluke voltmeter to measure initial voltage as shown in Figure 20. A LabVIEW program was written to take voltage and current as an input and multiply it to convert to total power. The block diagram for this program can be seen in Figure 21. This program was used in combination with the MyRIO measurement device connected to a basic circuit.

Figure 20: MyRIO and Fluke Voltmeter

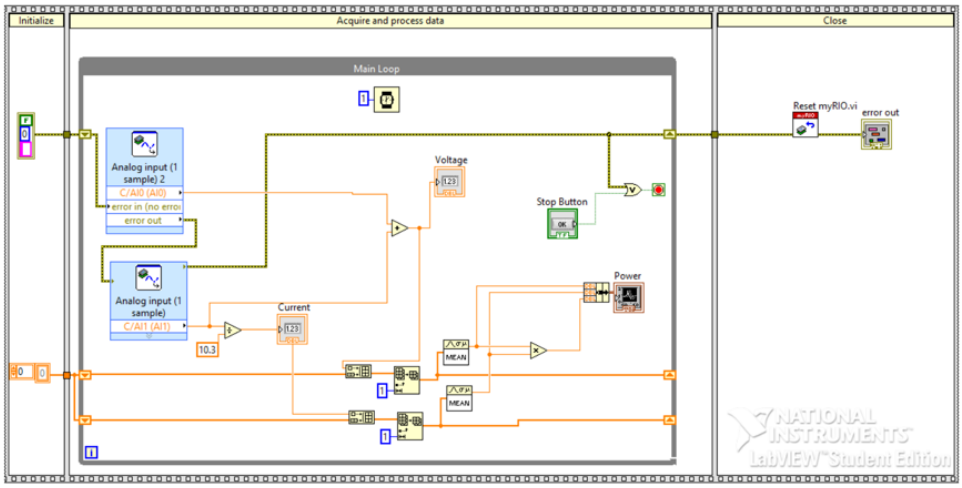

Figure 21: LabVIEW Program Block Diagram

The MyRIO does not measure current and power input directly, only voltage. To make the MyRIO work for current and power measurements a circuit was needed to take current measurements. The circuit used, shown in Figure 22, is a voltage divider circuit.

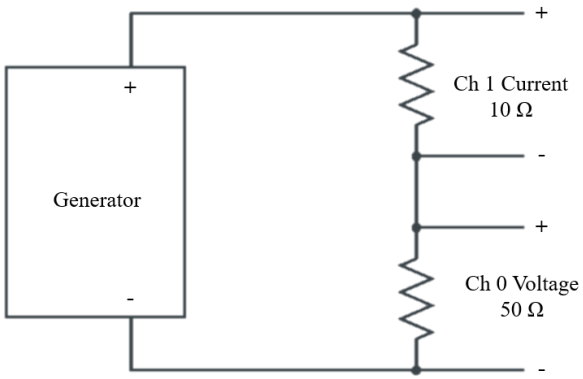

Figure 22: Voltage Divider Circuit used to Measure Power

To connect the circuit in Figure 22 to the MyRIO, a breadboard was used to build the circuit, shown in Figure 23. Connecting wires, shown in Figure 23, were used to make the connection from the generator wires to the breadboard, and from the breadboard to the MyRIO.

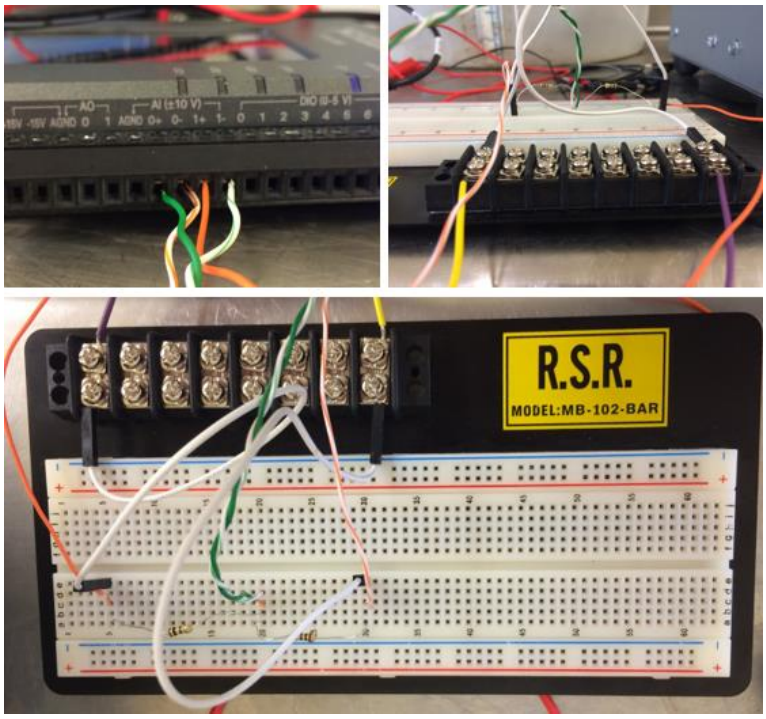

Figure 23: Breadboard and Connection Wires to the MyRIO

With the circuit hooked up to the MyRIO the LabVIEW program, Figure 21, can successfully take voltage, current, and power data points and export them to an Excel file.

The testing facility's water tunnel was equipped with three pumps that moved water from one reservoir to another on opposite sides of the tunnel. The equipment available to measure the fluid velocity was a pitot tube set up to measure the stagnation and static pressure shown in Figure 24. The height difference displayed on the gauge was recorded and using the Bernoulli's equation, the fluid velocity was calculated.

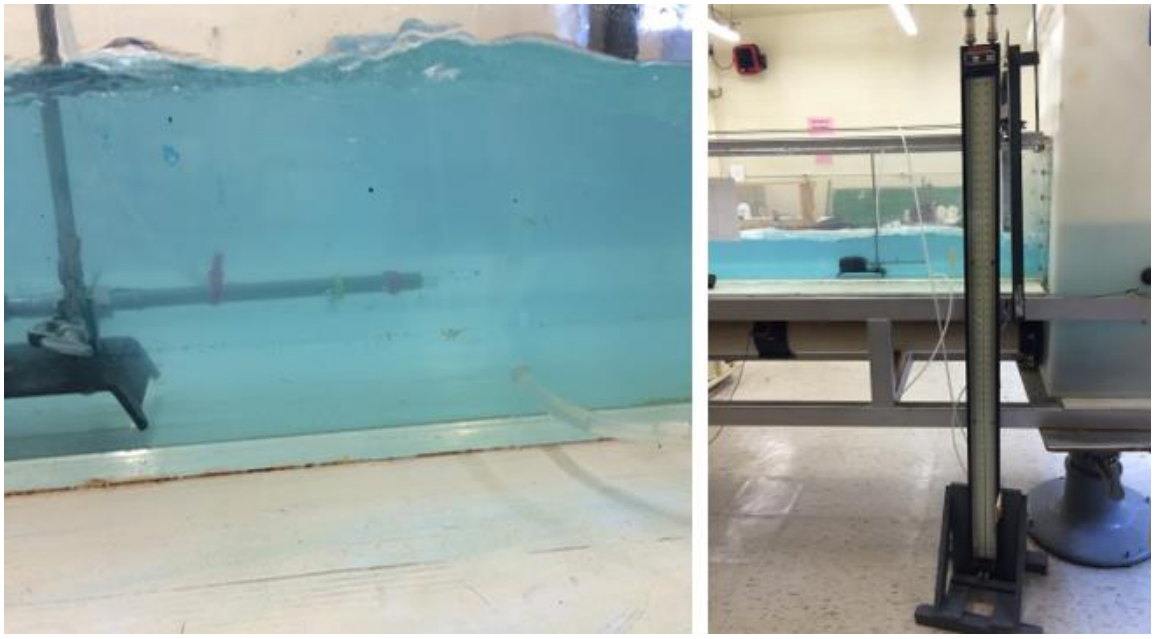

Figure 24: Pitot Tube and Measurement Gauge Set Up

To measure the number of rotations the HHA turns during the test a tachometer, shown in Figure 25, was used. The spinning attachment was placed on the end of the gear shaft. Three data points were taken and averaged for every test. With the RPMs for gear shaft the total RPMs of the generator can be calculated.

Figure 25: Tachometer Used to Measure RPM

2.2 Experiment Procedure and Explanation

The initial set up was similar for each test and with all of the equipment listed in the previous sections and the facility's water tunnel, experiment Parts 1 and 2 were completed. The conditions for Part 1 were to test each HHA design in a steady state, relatively laminar water flow that completely submerged the HHA prototypes. The conditions of Part 2 were to test three of the HHA designs in a steady state, turbulent water flow that did not submerge the HHA prototypes. The goal of both Parts 1 and 2 was to test each HHA prototype and determine the best HHA design out of the designs presented. Each experiment test involved setting up the mounting bracket with a different HHA prototype and lowering it into the water tunnel. The facility's water tunnel required three operational pumps and movable leveling gates for the entrance and exit of the flow. The initial objective was to test the HHA prototypes in a completely submerged setting, but the pump capabilities of the water tunnel could not completely submerge the HHA prototype. For Part 1 of the experiment, each gate was lowered to the appropriate height to replicate mostly laminar flow with enough depth to cover the majority of the HHA prototype. Readings were taken from the pitot tube located upstream in the water tunnel to determine water velocity. A schematic for experiment set up is shown for Part 1 in Figure 26.

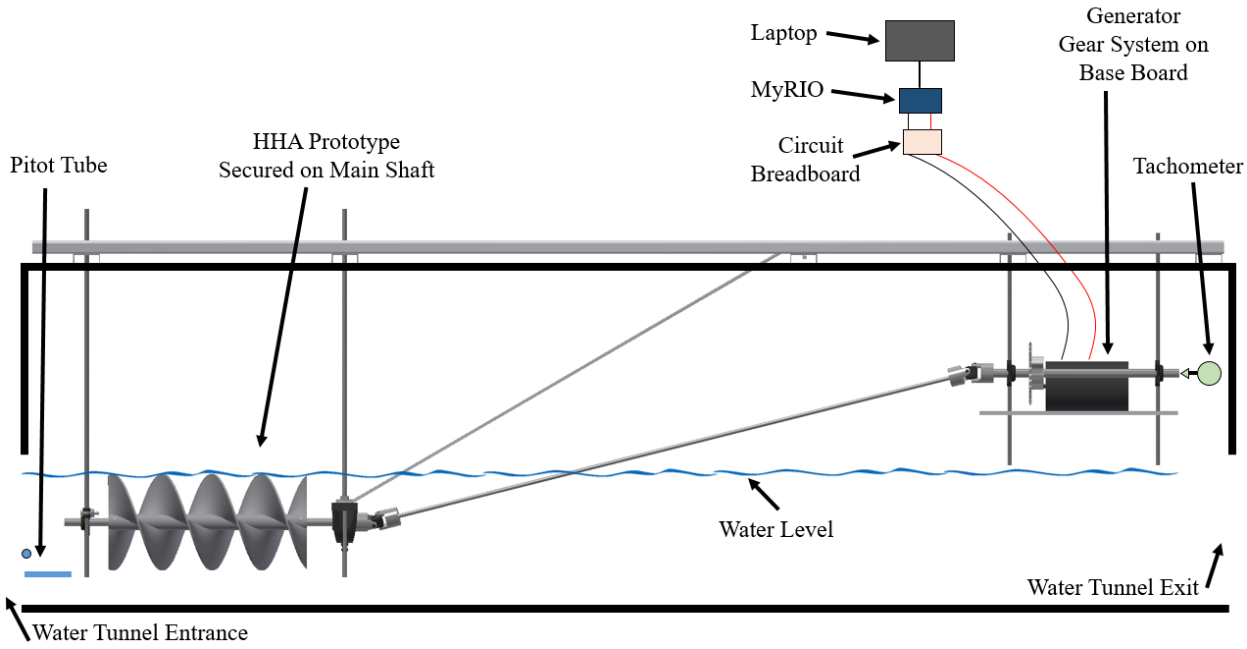

Figure 26: Experiment Part 1 Set Up

The mounting bracket assembly held the HHA prototype securely in the tunnel without any linear motion. Keeping the HHA prototype from moving backwards in the water flow was important for the set up to allow prototype to collect as much energy as possible. The generator on the base board was hooked up to the circuit on the breadboard which was hooked up the MyRIO and a laptop. The laptop allowed for a portable and functional system. Once the HHA prototype had reached steady state in the water flow, the tachometer was used to measure the rotations of the gear shaft and the MyRIO LabVIEW program was started. Each test ran for five minutes to obtain steady state and voltage, current, and power values were recorded for the last minute taking data every 10 milliseconds for a total of 1,000 values. The data from the program was downloaded onto the laptop through an Excel file and saved.

This procedure was repeated for all HHA prototype models at the same water velocity, Table 2 is a summary of the combinations tested for the Part 1 of the experiment.

Table 2: Experiment Part 1

Test #	HHA Prototype	Pitch (inches)	Blade Revolutions	PVC Pipe Attachment	Edge Feature	Water Velocity (ft/sec)
1	Auger 1	4	3	Y	N	3.5
2	Auger 2	6	2	Y	N	3.5
3	Auger 3	4	3	N	Y	3.5
4	Auger 4	6	2	N	Y	3.5
5	Auger 1	4	3	N	N	3.5
6	Auger 2	6	2	N	N	3.5

Part 2 of the experiment had the same set up procedure as Part 1, with the only difference being water velocity. To create a faster velocity in the water tunnel the entrance gate was lowered and the exit gate was raised all the way up to allow the water to exit quickly. This created an extremely turbulent flow and the pitot tube could not measure water velocity in this state. Instead, a float was dropped down into the beginning of the tunnel and timed using a stopwatch until it reached the end of the tunnel's known length. This velocity measurement was taken three times and averaged. The water tunnel's capacity could not completely fully submerge the HHA prototypes and maintain the fast velocity. The Part 2 test set up can be seen in the schematic shown in Figure 27.

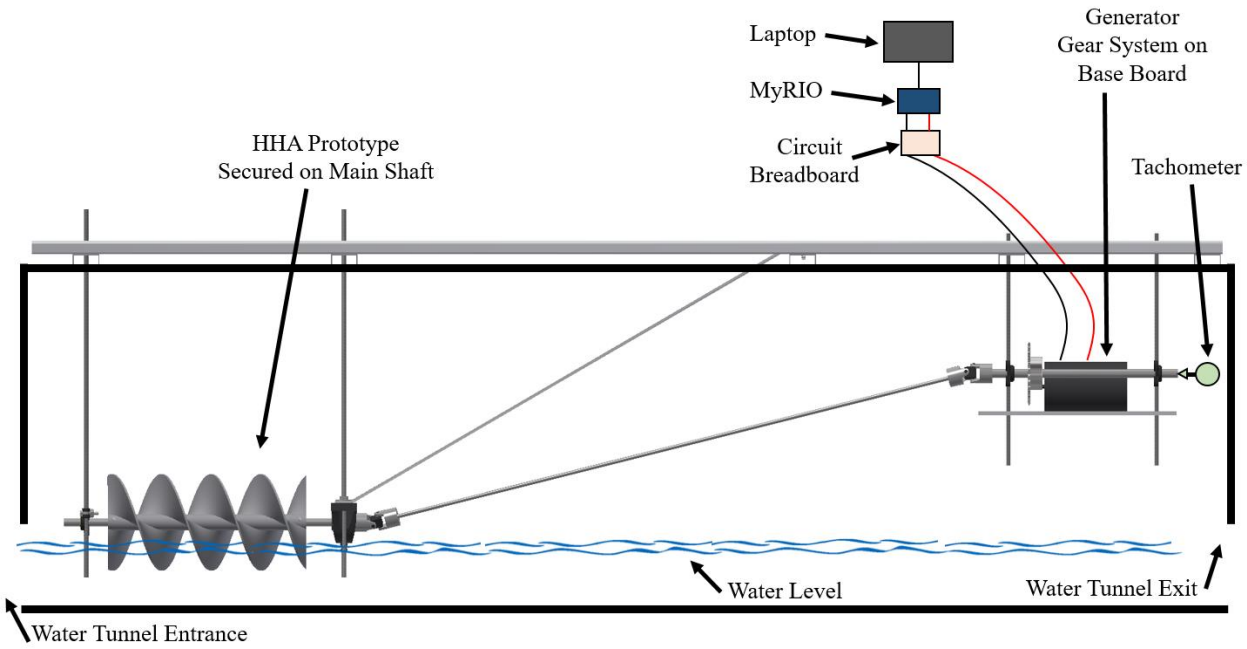

Figure 27: Experiment Part 2 Set Up

Three tests were done for Part 2 and only three of the HHA prototype models were used, the summary table is shown in Table 3 for Part 2.

Table 3: Experiment Part 2

Test #	HHA Prototype	Pitch (inches)	Blade Revolutions	PVC Pipe Attachment	Edge Feature	Water Velocity (ft/sec)
1	Auger 1	4	3	N	N	5
2	Auger 2	6	2	N	N	5
3	Auger 4	6	2	N	Y	5

Each test for both Part 1 and 2 ran for five minutes to reach steady state and data was taken during the last minute after steady state had been reached for a total of approximately 1,000 data points for each test. Water velocity was recorded using the pitot tube and using the tachometer, rotations per minute were measured three times, averaged and recorded for each test. HHA surface area covered in water was also visually observed and recorded for each test. This

experiment consisted of Part 1 and 2 that tested several combinations of HHA prototypes with different features.

CHAPTER 3: Experimental Results and Comparison

3.1 Calculations for Constants

This chapter will discuss all of Part 1 and Part 2 test results in detail. Recalling Table 2: Experiment Part 1Table 2 and Table 3 there were several combinations of HHA prototypes and design features. Even with different design characteristics, the water velocity, gear ratio, and generator velocity calculations are the same for all tests in Part 1 and Part 2. These calculations will be discussed once because of the identical processes for each test run. Parts 1 and 2 will be discussed in the following sections.

3.1.1 Part 1 Water Velocity Calculation

The water velocity for Part 1 was calculated using Bernoulli's equation using the pitot tube and height gauge. This method was used for Part 1 because it is only successful during a relatively laminar flow. Bernoulli's Equation is as follows where, P is the static pressure, P_0 is the stagnation pressure, ρ is the density of water, and v is the water velocity

$$P_0 = P + \frac{1}{2}\rho v^2. \tag{20}$$

Before the water tunnel was turned on, the zero points on the height gauge were noted. After the water tunnel had been on and the flow had reached steady state, the height measurements were taken from the gauge. The difference in height between the two readings for stagnation pressure and static pressure were taken and the total height difference was converted to pascals. The readings taken for the experiment Part 1 are in Table 4.

Table 4: Part 1 Water Velocity Calculation Variables

Density of Water at 40°C (ρ)	1000 kg/m^3
Change in Stagnation Pressure (P_0)	4 inches
Change in Static Pressure (P)	1.7 inches
Total Pressure Change (ΔP)	2.3 inches
Total Pressure (P)	573 Pa

Solving Eq. 20 for water velocity using the total pressure, 573 Pa, calculated in Table 4

$$v = \sqrt{\frac{(P_0 - P) * 2}{\rho}} = \sqrt{\frac{573 * 2}{1000}} = 1.07\ m/s$$

The water velocity for experiment Part 1 was $1.07\ m/s\ or\ 3.5\ ft/s$.

3.1.2 Part 2 Water Velocity Calculation

The water velocity for Part 2 was calculated using a time and distance recording process. This process was used for Part 2 because the flow was not laminar and the pitot tubes do not work under turbulent conditions. To calculate the water velocity, the length of the water tunnel was recorded, a float was dropped in the tunnel at the entrance, and the float was timed as it traveled the entire distance of the tunnel. This was done three times and the times were averaged to get an average water velocity shown in Table 5.

Table 5: Part 2 Water Velocity Calculation Variables

Water Tunnel Length	15 ft
Time 1	3.2 seconds
Time 2	3.0 seconds
Time 3	2.9 seconds
Average Time	3.03 seconds

The water velocity for experiment Part 1 was $1.52\ m/s\ or\ 5.0\ ft/s$.

3.1.3 Gear Ratio Calculation

The gear ratio calculation is identical for both Parts 1 and 2 as the gears never change. Calculating the gear ratio is necessary to determine the total number of rotations per minute for the generator. The number of teeth the gears had were needed to calculate the gear ratio for the gear system that drives the generator. There were two gears on the system, a small gear connected to the generator shaft and a big gear on the gear shaft connected by a small chain loop.

$$Number\ of\ Teeth\ Small\ Gear = 11$$

$$Number\ of\ Teeth\ Big\ Gear = 40$$

$$Gear\ Ratio = \frac{Number\ of\ Teeth\ Big\ Gear}{Number\ of\ Teeth\ Small\ Gear} = \frac{40}{11} = 3.64 \quad (21)$$

3.1.4 Generator Shaft Velocity

The gear shaft rotations per minute were recorded using the tachometer for each test for both Part 1 and 2. Multiplying the gear shaft rotations per minute recorded by the tachometer by the gear ratio produces the generator shaft rotations per minute. With the rotations per minute of the generator shaft, the angular velocity and linear velocity of the generator can be calculated. To calculate angular velocity, the rotations per minute must be converted to radians per second.

$$\frac{Rotations}{Minute} * 2\pi \frac{Radians}{Revolution} * \frac{1}{60}\frac{Minute}{Seconds} = \frac{Radians}{Second} = Angular\ Velocity\ (\omega) \quad (22)$$

3.2 Experiment Part 1

This section will discuss all experimental results for Part 1. All HHA designs and attachment combinations can be referenced from Table 2. For specific HHA dimensions and descriptions Table 1 should be reviewed. As stated in the previous section, the water velocity, gear ratio and generator shaft velocity were calculated the same for each test and will not be discussed in detail in this section and only values will be examined.

3.2.1 Part 1 Test 1

Test 1 consisted of HHA design 1 with the PVC pipe attachment, see Table 6 for all features. The standard test set up and procedure for Part 1 discussed in Chapter 2.2 was followed for data collection. The experiment set up for Test 1 can be seen below in Figure 28.

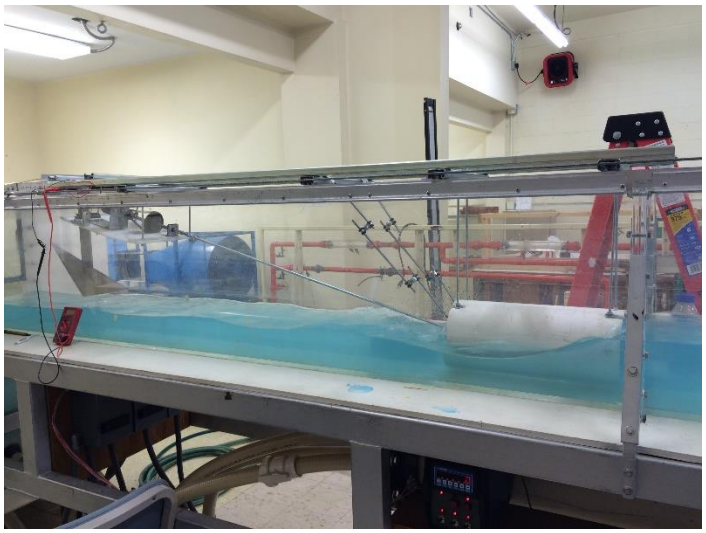

Figure 28: Part 1 Test 1 Experiment Set Up

The HHA prototype successfully turned in the water and data was collected. All of the data collected included: water velocity, rotations per minute of the gear shaft and generator shaft, surface area covered by water of the front and back of the prototype, and voltage, current, and power measurements. This data is displayed in the results summary

Table 7.

Table 6: Part 1 Test 1 HHA Design Features

HHA Prototype Design	Pitch (inches)	Blade Revolutions	PVC Pipe Attachment	Edge Feature	Water Velocity (ft/sec)
Auger 1	4	3	Y	N	3.5

Table 7: Part 1 Test 1 Results

Gear Shaft RPM	Generator Shaft RPM	% Area Covered by Water		Average Voltage (volts)	Average Current (amps)	Average Power (watts)
		Front	Back			
155	465	100	60	2.994	0.049	0.149

With the data collected, the theory from Section 1.2.3 was used to determine the HHA prototype power efficiency. To use these equations all of the variables must be either calculated or defined, Table 8 defines each variable used for the efficiency calculations.

Table 8: Part 1 Test 1 Power & Efficiency Variables

Variable	Value	Units
Water Density (ρ)	1.940	slugs/ft^3
% Front Area Submerged	100%	-
% Back Area Submerged	60%	-
Average % Area Submerged	80%	-
HHA Length (L_b)	1.0	ft
HHA Outer Radius (R_o)	0.25	ft
HHA Hub Radius (R_i)	0.041	ft
HHA Total Submerged Area (A_b)	0.166	ft^2
HHA Effective Radius (R)	0.166	ft
Coefficient of Drag (C_D)	1.6	-
Relative Velocity (V_r)	0.795	ft/s
Water Velocity (V_C)	3.5	ft/s
Blade Velocity (V_b)	2.704	ft/s

HHA Angular Velocity (ω)	16.231	rad/s
HHA RPM	155	RPM

The lines 1 through 7, 10, 12, and 16 in Table 8 were variables recorded during the experiment. The other variables were calculated using equations listed in Chapter 1.2.3. The HHA total submerged area, A_b, was calculated by using Eq. 11

$$A_b = L_b * (R_o - R_i) = 1.0 * (0.25 - 0.0417) * 80\% = 0.166\ ft^2.$$

The HHA effective radius, R, was calculated using Eq. 10

$$R = (R_o - R_i) * 80\% = 0.25 - 0.0417 = 0.166\ ft.$$

The HHA angular velocity, ω, was calculated using Eq. 22

$$155\ RPM * 2\pi * \frac{1}{60} = 16.231\ rad/s.$$

The HHA blade velocity, V_b, was calculated using Eq. 10

$$V_b = \omega * R = 2.704\ ft/s.$$

The relative velocity, V_r, was calculated using Eq. 8

$$V_r = (V_c - V_b) = 3.5 - 2.7048 = 0.795\ ft/s.$$

With all of the variables calculated, the force exerted on the blade, F_D, of the HHA is determined by Eq. 7

$$F_D = \frac{1}{2} * \rho * V_r^2 * A_b * C_D = \frac{1}{2} * 1.94 * 0.795^2 * 0.166 * 1.6 = 0.163\ lbf.$$

To calculate the potential power, P_T, produced by the HHA Eq. 12 is used

$$P_T = F_D * V_b = 0.163 * 2.704 = 0.442\ watts.$$

To calculate the hydraulic efficiency, the torque, T, acting on the HHA shaft is determined using Eq. 16 and the mechanical power, P_M, is calculated using Eq. 17

$$T = F_D * R = 0.027\ lbf * ft$$

$$P_M = \omega * T = 16.231 * 0.027 = 0.442\ watts.$$

The theoretical power produced by the water flow, P_{Th}, is the other necessary component to calculate hydraulic efficiency and is calculated using Eq. 15

$$P_{Th} = \frac{1}{2} * \rho * A_b * C_D * {V_c}^3 = \frac{1}{2} * 1.940 * 0.166 * 1.6 * 3.5^3 = 11.088\ watts.$$

With these values, the hydraulic efficiency, η_{hyd}, can be calculated using Eq. 18

$$\eta_{hyd} = \frac{P_M}{P_{Th}} = \frac{0.442}{11.088} = 4.0\%.$$

This calculated efficiency compares the power in the water flow to the potential power of the HHA. The amount of power the HHA prototype produced from the water flow during Test 1 was recorded and compared to the potential power in Eq. 12. The efficiency of the HHA prototype design for Test 1 is calculated using Eq. 20

$$\eta_A = \frac{P_{Ex}}{P_T} = \frac{0.149}{0.442} = 34\%.$$

With all of the equations calculated using the power recorded from Test 1, the power and efficiencies are summarized in Table 9 below.

Table 9: Part 1 Test 1 Power & Efficiency Values

Power & Efficiencies	Value	Units
Force Exerted on HHA Blade (F_D)	0.163	lbf
Potential Power Produced by the HHA (P_T)	0.442	watts
Theoretical Power of the Water Velocity(P_{Th})	11.088	watts
Torque Acting on HHA Shaft (T)	0.027	lbf*ft
Mechanical Power Produced by the HHA (P_M)	0.442	watts
Hydraulic Efficiency of the HHA (η_{hyd})	4%	-
Experimental Power Produced by the HHA (P_{Ex})	0.149	watts
Actual Power Efficiency of the HHA (η_A)	34%	-

3.2.2 Part 1 Test 2

Test 2 consisted of HHA design 2 with the PVC pipe attachment, see

Table 10 for all features. The test set up and procedure for Part 1 discussed in Section 2.2 was followed. The experiment set up and data collected can be seen below in Figure 29 and Table 11, respectively.

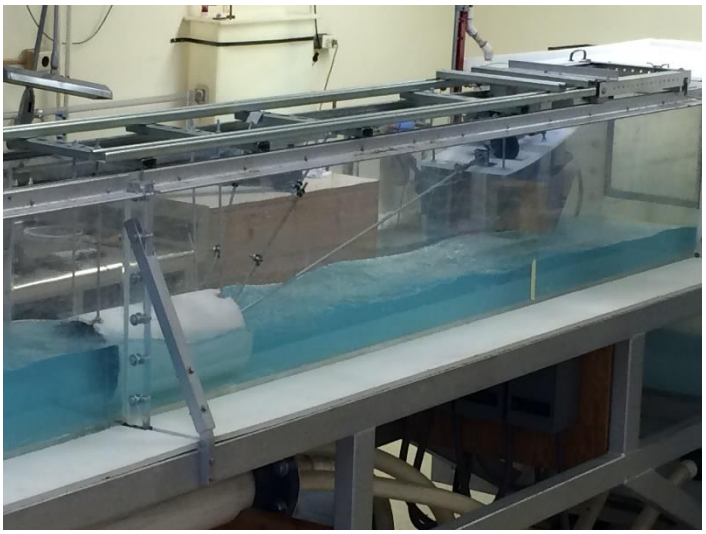

Figure 29: Part 1 Test 2 Experiment Set Up

Table 10: Part 1 Test 2 HHA Design Features

HHA Prototype Design	Pitch (inches)	Blade Revolutions	PVC Pipe Attachment	Edge Feature	Water Velocity (ft/sec)
Auger 2	6	2	Y	N	3.5

Table 11: Part 1 Test 2 Results

Gear Shaft RPM	Generator Shaft RPM	% Area Covered by Water		Average Voltage (volts)	Average Current (amps)	Average Power (watts)
		Front	Back			
153	556	100	60	2.871	0.047	0.137

All of the same equations that were used for Test 1 were used to calculate the variables for Test 2. These variables are shown below in Table 12 and the calculated power and efficiencies are in Table 13.

Table 12: Part 1 Test 2 Power & Efficiency Variables

Variable	Value	Units
Water Density (ρ)	1.940	slugs/ft^3
% Front Area Submerged	100%	-
% Back Area Submerged	60%	-
Average % Area Submerged	80%	-
HHA Length (L_b)	1.0	ft
HHA Outer Radius (R_o)	0.25	ft
HHA Hub Radius (R_i)	0.041	ft
HHA Total Submerged Area (A_b)	0.166	ft^2
HHA Effective Radius (R)	0.166	ft
Coefficient of Drag (C_D)	1.6	-
Relative Velocity (V_r)	0.830	ft/s
Water Velocity (V_C)	3.5	ft/s
Blade Velocity (V_b)	2.669	ft/s
HHA Angular Velocity (ω)	16.022	rad/s
HHA RPM	153	RPM

Table 13: Part 1 Test 2 Power & Efficiency Values

Power & Efficiencies	Value	Units
Force Exerted on HHA Blade (F_D)	0.178	lbf
Potential Power Produced by the HHA (P_T)	0.475	watts
Theoretical Power of the Water Velocity(P_{Th})	11.088	watts
Torque Acting on HHA Shaft (T)	0.029	lbf*ft
Mechanical Power Produced by the HHA (P_M)	0.475	watts
Hydraulic Efficiency of the HHA (η_{hyd})	4.3%	-
Experimental Power Produced by the HHA (P_{Ex})	0.137	watts
Actual Power Efficiency of the HHA (η_A)	29%	-

3.2.3 Part 1 Test 3

Test 3 consisted of HHA design 3, see Table 14 for all features. The standard test set up and procedure for Part 1 discussed in Section 2.2 was followed for data collection. The experiment set up and data collected for Test 3 can be seen below in Figure 30 and Table 15, respectively. All of the same equations that were used for Test 1 were used to calculate the variables for Test 3. These variables are shown below in Table 16 and the calculated power and efficiencies are in Table 17.

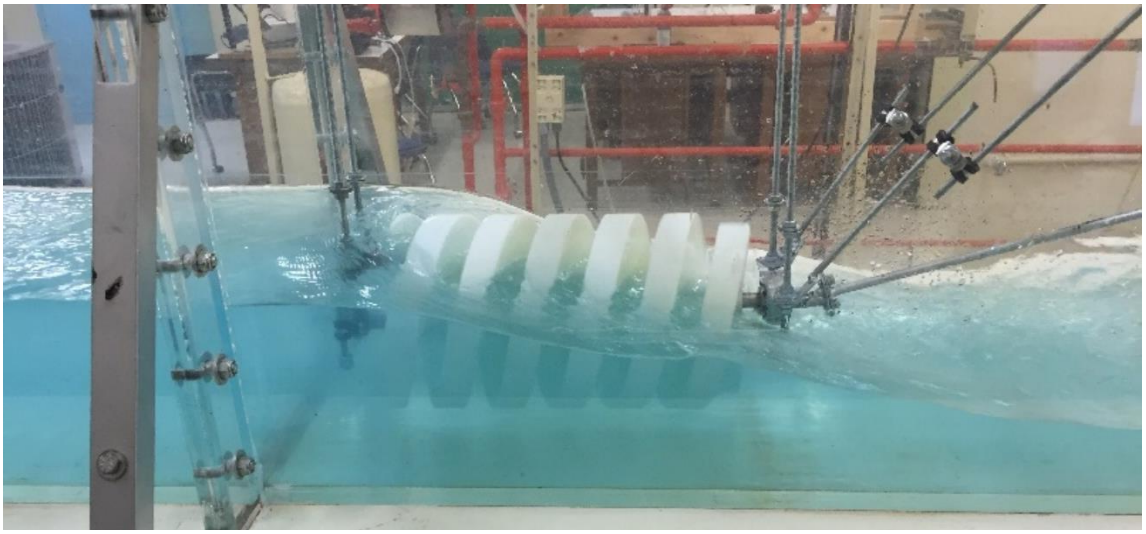

Figure 30: Part 1 Test 3 Experiment Set Up

Table 14: Part 1 Test 3 HHA Design Features

HHA Prototype Design	Pitch (inches)	Blade Revolutions	PVC Pipe Attachment	Edge Feature	Water Velocity (ft/sec)
Auger 3	4	3	N	Y	3.5

Table 15: Part 1 Test 3 Results

Gear Shaft RPM	Generator Shaft RPM	% Area Covered by Water		Average Voltage (volts)	Average Current (amps)	Average Power (watts)
		Front	Back			
135	491	100	45	2.506	0.041	0.104

Table 16: Part 1 Test 3 Power & Efficiency Variables

Variable	Value	Units
Water Density (ρ)	1.940	slugs/ft^3
% Front Area Submerged	100%	-
% Back Area Submerged	40%	-
Average % Area Submerged	70%	-
HHA Length (L_b)	1.0	ft
HHA Outer Radius (R_o)	0.25	ft
HHA Hub Radius (R_i)	0.041	ft
HHA Total Submerged Area (A_b)	0.145	ft^2
HHA Effective Radius (R)	0.145	ft
Coefficient of Drag (C_D)	1.6	-
Relative Velocity (V_r)	1.438	ft/s
Water Velocity (V_C)	3.5	ft/s
Blade Velocity (V_b)	2.061	ft/s
HHA Angular Velocity (ω)	14.137	rad/s
HHA RPM	135	RPM

Table 17: Part 1 Test 3 Power & Efficiency Values

Power & Efficiencies	Value	Units
Force Exerted on HHA Blade (F_D)	0.468	lbf
Potential Power Produced by the HHA (P_T)	0.965	watts
Theoretical Power of the Water Velocity(P_{Th})	9.702	watts
Torque Acting on HHA Shaft (T)	0.068	lbf*ft
Mechanical Power Produced by the HHA (P_M)	0.965	watts
Hydraulic Efficiency of the HHA (η_{hyd})	10%	-
Experimental Power Produced by the HHA (P_{Ex})	0.104	watts
Actual Power Efficiency of the HHA (η_A)	11%	-

3.2.4 Part 1 Test 4

Test 4 consisted of HHA design 4, see Table 18 for all features. The standard test set up and procedure for Part 1 discussed in Section 2.2 was followed for data collection. The experiment set up and data collected for Test 4 can be seen below in Figure 31 and Table 19Table 15, respectively. All of the same equations that were used for Test 1 were used to calculate the variables for Test 4. These variables are shown below in Table 20Table 16 and the calculated power and efficiencies are in Table 21Table 17.

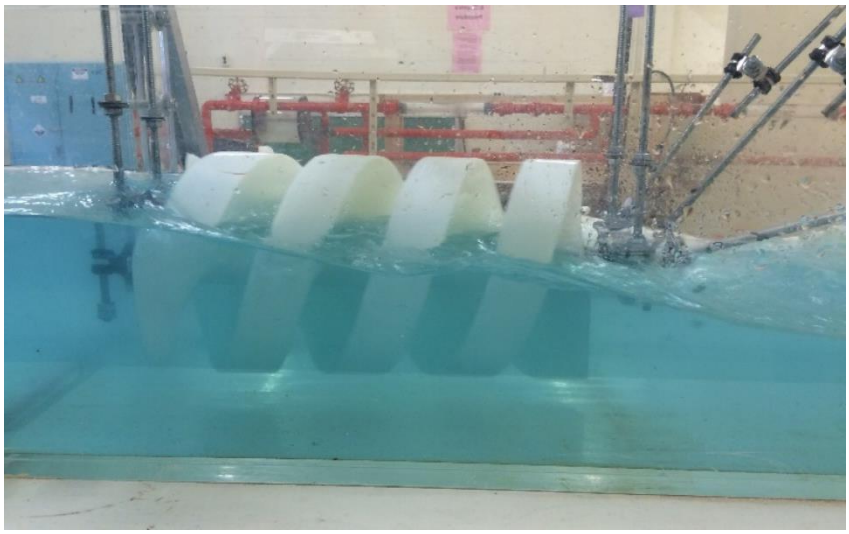

Figure 31: Part 1 Test 4 Experiment Set Up

Table 18: Part 1 Test 4 HHA Design Features

HHA Prototype Design	Pitch (inches)	Blade Revolutions	PVC Pipe Attachment	Edge Feature	Water Velocity (ft/sec)
Auger 4	6	2	N	Y	3.5

Table 19: Part 1 Test 4 Results

Gear Shaft RPM	Generator Shaft RPM	% Area Covered by Water		Average Voltage (volts)	Average Current (amps)	Average Power (watts)
		Front	Back			
133	484	95	50	2.513	0.041	0.104

Table 20: Part 1 Test 4 Power & Efficiency Variables

Variable	Value	Units
Water Density (ρ)	1.940	slugs/ft^3
% Front Area Submerged	95%	-
% Back Area Submerged	50%	-
Average % Area Submerged	73%	-
HHA Length (L_b)	1.0	ft
HHA Outer Radius (R_o)	0.25	ft
HHA Hub Radius (R_i)	0.041	ft
HHA Total Submerged Area (A_b)	0.151	ft^2
HHA Effective Radius (R)	0.151	ft
Coefficient of Drag (C_D)	1.6	-
Relative Velocity (V_r)	1.396	ft/s
Water Velocity (V_C)	3.5	ft/s
Blade Velocity (V_b)	2.103	ft/s
HHA Angular Velocity (ω)	13.927	rad/s
HHA RPM	133	RPM

Table 21: Part 1 Test 4 Power & Efficiency Values

Power & Efficiencies	Value	Units
Force Exerted on HHA Blade (F_D)	0.457	lbf
Potential Power Produced by the HHA (P_T)	0.961	watts
Theoretical Power of the Water Velocity(P_{Th})	10.049	watts
Torque Acting on HHA Shaft (T)	0.069	lbf*ft
Mechanical Power Produced by the HHA (P_M)	0.961	watts
Hydraulic Efficiency of the HHA (η_{hyd})	9.6%	-
Experimental Power Produced by the HHA (P_{Ex})	0.104	watts
Actual Power Efficiency of the HHA (η_A)	11%	-

3.2.5 Part 1 Test 5

Test 5 consisted of HHA design 1, see Table 22 for all features. The standard test set up and procedure for Part 1 discussed in Section 2.2 was followed for data collection. The experiment set up and data collected for Test 5 can be seen below in Figure 32 and Table 23Table 19Table 15, respectively. All of the same equations that were used for Test 1 were used to calculate the variables for Test 5. These variables are shown below in Table 24Table 16 and the calculated power and efficiencies are in Table 25Table 17.

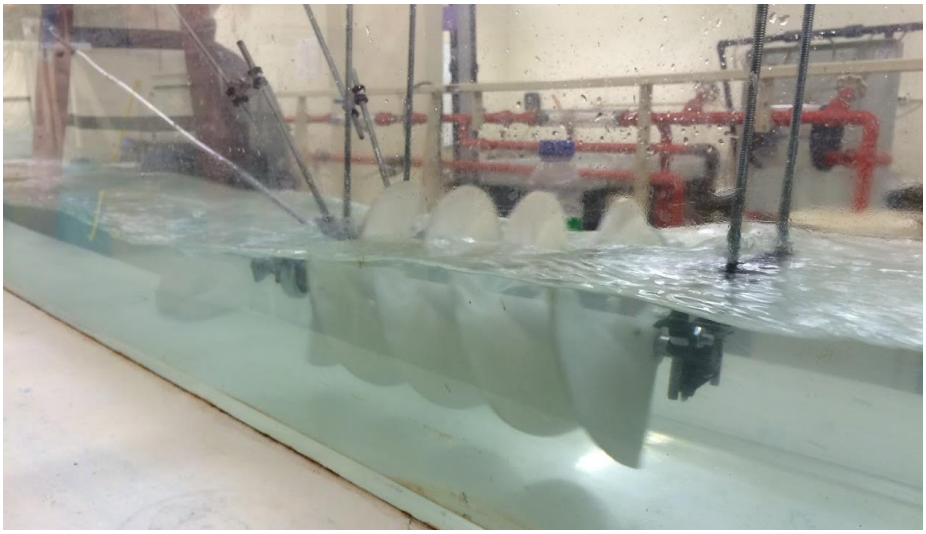

Figure 32: Part 1 Test 5 Experiment Set Up

Table 22: Part 1 Test 5 HHA Design Features

HHA Prototype Design	Pitch (inches)	Blade Revolutions	PVC Pipe Attachment	Edge Feature	Water Velocity (ft/sec)
Auger 1	4	3	N	N	3.5

Table 23: Part 1 Test 5 Results

Gear Shaft RPM	Generator Shaft RPM	% Area Covered by Water		Average Voltage (volts)	Average Current (amps)	Average Power (watts)
		Front	Back			
158	575	95	45	3.066	0.050	0.156

Table 24: Part 1 Test 5 Power & Efficiency Variables

Variable	Value	Units
Water Density (ρ)	1.940	slugs/ft^3
% Front Area Submerged	95%	-
% Back Area Submerged	45%	-
Average % Area Submerged	70%	-
HHA Length (L_b)	1.0	ft
HHA Outer Radius (R_o)	0.25	ft
HHA Hub Radius (R_i)	0.041	ft
HHA Total Submerged Area (A_b)	0.145	ft^2
HHA Effective Radius (R)	0.145	ft
Coefficient of Drag (C_D)	1.6	-
Relative Velocity (V_r)	1.087	ft/s
Water Velocity (V_C)	3.5	ft/s
Blade Velocity (V_b)	2.412	ft/s
HHA Angular Velocity (ω)	16.545	rad/s
HHA RPM	158	RPM

Table 25: Part 1 Test 5 Power & Efficiency Values

Power & Efficiencies	Value	Units
Force Exerted on HHA Blade (F_D)	0.267	lbf
Potential Power Produced by the HHA (P_T)	0.645	watts
Theoretical Power of the Water Velocity(P_{Th})	9.702	watts
Torque Acting on HHA Shaft (T)	0.039	lbf*ft
Mechanical Power Produced by the HHA (P_M)	0.645	watts
Hydraulic Efficiency of the HHA (η_{hyd})	6.7%	-
Experimental Power Produced by the HHA (P_{Ex})	0.156	watts
Actual Power Efficiency of the HHA (η_A)	24%	-

3.2.6 Part 1 Test 6

Test 6 consisted of HHA design 1, see Table 26 for all features. The standard test set up and procedure for Part 1 discussed in Section 2.2 was followed for data collection. The experiment set up is identical to Figure 32, but with Auger 2 instead of Auger 1. The data collected for Test 6 can be seen in Figure 31Table 27. All of the same equations that were used for Test 1 were used to calculate the variables for Test 6. These variables are shown below in Table 28Table 16 and the calculated power and efficiencies are in Table 29Table 17.

Table 26: Part 1 Test 6 HHA Design Features

HHA Prototype Design	Pitch (inches)	Blade Revolutions	PVC Pipe Attachment	Edge Feature	Water Velocity (ft/sec)
Auger 2	6	2	N	N	3.5

Table 27: Part 1 Test 6 Results

Gear Shaft RPM	Generator Shaft RPM	% Area Covered by Water		Average Voltage (volts)	Average Current (amps)	Average Power (watts)
		Front	Back			
155	564	85	60	3.001	0.049	0.150

Table 28: Part 1 Test 6 Power & Efficiency Variables

Variable	Value	Units
Water Density (ρ)	1.940	slugs/ft^3
% Front Area Submerged	85%	-
% Back Area Submerged	60%	-
Average % Area Submerged	73%	-
HHA Length (L_b)	1.0	ft
HHA Outer Radius (R_o)	0.25	ft
HHA Hub Radius (R_i)	0.041	ft
HHA Total Submerged Area (A_b)	0.151	ft^2
HHA Effective Radius (R)	0.151	ft
Coefficient of Drag (C_D)	1.6	-
Relative Velocity (V_r)	1.048	ft/s
Water Velocity (V_C)	3.5	ft/s
Blade Velocity (V_b)	2.451	ft/s
HHA Angular Velocity (ω)	16.231	rad/s
HHA RPM	155	RPM

Table 29: Part 1 Test 6 Power & Efficiency Values

Power & Efficiencies	Value	Units
Force Exerted on HHA Blade (F_D)	0.257	lbf
Potential Power Produced by the HHA (P_T)	0.631	watts
Theoretical Power of the Water Velocity(P_{Th})	10.049	watts
Torque Acting on HHA Shaft (T)	0.038	lbf*ft
Mechanical Power Produced by the HHA (P_M)	0.631	watts
Hydraulic Efficiency of the HHA (η_{hyd})	6.3%	-
Experimental Power Produced by the HHA (P_{Ex})	0.150	watts
Actual Power Efficiency of the HHA (η_A)	24%	-

3.3 Experiment Part 2

This section discusses the results for Part 2 of the experiment. The procedure and set up are discussed in Section 2.2 and the all of the HHA designs and attachment combinations can be referenced from Table 3. For specific HHA dimensions and descriptions Table 1 should be reviewed. As stated previously, the water velocity, gear ratio and generator shaft velocity were calculated the same for each test and will not be discussed in detail in this section and only values will be examined.

3.3.1 Part 2 Test 1

HHA design 1 was used for Test 1, see Table 30 for the design features. The test set up and data collection procedure described in Section 2.2 was used. Part two involved a faster velocity and the testing facilities water tunnel was not able to produce the increased velocity with a depth more than a few inches. Figure 27 shows the lower water level on the HHA prototype and the set up was identical to Figure 33 except Auger 1 was used. The data collected for Test 1 can be seen in Figure 31Table 31. All of the same equations that were used for Part 1 Test 1 were used to calculate the variables for Test 1. These variables are shown below in Table 32Table 16 and the calculated power and efficiencies are in Table 33Table 17.

Table 30: Part 2 Test 1 HHA Design Features

HHA Prototype Design	Pitch (inches)	Blade Revolutions	PVC Pipe Attachment	Edge Feature	Water Velocity (ft/sec)
Auger 1	4	3	N	N	5.0

Table 31: Part 2 Test 1 Results

Gear Shaft RPM	Generator Shaft RPM	% Area Covered by Water		Average Voltage (volts)	Average Current (amps)	Average Power (watts)
		Front	Back			
170	618	40	40	3.303	0.054	0.182

Table 32: Part 2 Test 1 Power & Efficiency Variables

Variable	Value	Units
Water Density (ρ)	1.940	slugs/ft^3
% Front Area Submerged	40%	-
% Back Area Submerged	40%	-
Average % Area Submerged	40%	-
HHA Length (L_b)	1.0	ft
HHA Outer Radius (R_o)	0.25	ft
HHA Hub Radius (R_i)	0.041	ft
HHA Total Submerged Area (A_b)	0.083	ft^2
HHA Effective Radius (R)	0.083	ft
Coefficient of Drag (C_D)	1.6	-
Relative Velocity (V_r)	3.516	ft/s
Water Velocity (V_C)	5.0	ft/s
Blade Velocity (V_b)	1.483	ft/s
HHA Angular Velocity (ω)	17.802	rad/s
HHA RPM	170	RPM

Table 33: Part 2 Test 1 Power & Efficiency Values

Power & Efficiencies	Value	Units
Force Exerted on HHA Blade (F_D)	1.599	lbf
Potential Power Produced by the HHA (P_T)	2.372	watts
Theoretical Power of the Water Velocity(P_{Th})	16.164	watts
Torque Acting on HHA Shaft (T)	0.133	lbf*ft
Mechanical Power Produced by the HHA (P_M)	2.372	watts
Hydraulic Efficiency of the HHA (η_{hyd})	14.7%	-
Experimental Power Produced by the HHA (P_{Ex})	0.182	watts
Actual Power Efficiency of the HHA (η_A)	8%	-

3.3.2 Part 2 Test 2

HHA design 2 was used for Test 2, see Table 34 for the design features. The test set up and data collection procedure described in Section 2.2 was used. Part two involved a faster velocity and the testing facilities water tunnel was not able to produce the increased velocity with a depth more than a few inches. Figure 27 shows the lower water level on the HHA prototype and the set up was identical to Figure 33 except Auger 2 was used. The data collected for Test 2 can be seen in Figure 31Table 35. All of the same equations that were used for Part 1 Test 1 were used to calculate the variables for Test 2. These variables are shown below in Table 36Table 16 and the calculated power and efficiencies are in Table 37Table 17.

Table 34: Part 2 Test 2 HHA Design Features

HHA Prototype Design	Pitch (inches)	Blade Revolutions	PVC Pipe Attachment	Edge Feature	Water Velocity (ft/sec)
Auger 2	6	2	N	N	5.0

Table 35: Part 2 Test 2 Results

Gear Shaft RPM	Generator Shaft RPM	% Area Covered by Water		Average Voltage (volts)	Average Current (amps)	Average Power (watts)
		Front	Back			
231	840	30	40	4.759	0.080	0.385

Table 36: Part 2 Test 2 Power & Efficiency Variables

Variable	Value	Units
Water Density (ρ)	1.940	slugs/ft^3
% Front Area Submerged	30%	-
% Back Area Submerged	40%	-
Average % Area Submerged	35%	-
HHA Length (L_b)	1.0	ft
HHA Outer Radius (R_o)	0.25	ft
HHA Hub Radius (R_i)	0.041	ft
HHA Total Submerged Area (A_b)	0.072	ft^2
HHA Effective Radius (R)	0.072	ft
Coefficient of Drag (C_D)	1.6	-
Relative Velocity (V_r)	3.236	ft/s
Water Velocity (V_C)	5.0	ft/s
Blade Velocity (V_b)	1.763	ft/s
HHA Angular Velocity (ω)	24.190	rad/s
HHA RPM	231	RPM

Table 37: Part 2 Test 2 Power & Efficiency Values

Power & Efficiencies	Value	Units
Force Exerted on HHA Blade (F_D)	1.185	lbf
Potential Power Produced by the HHA (P_T)	2.090	watts
Theoretical Power of the Water Velocity(P_{Th})	14.143	watts
Torque Acting on HHA Shaft (T)	0.086	lbf*ft
Mechanical Power Produced by the HHA (P_M)	2.090	watts
Hydraulic Efficiency of the HHA (η_{hyd})	14.8%	-
Experimental Power Produced by the HHA (P_{Ex})	0.385	watts
Actual Power Efficiency of the HHA (η_A)	18%	-

3.3.3 Part 2 Test 3

HHA design 4 was used for Test 3, see Table 34 for the design features. The test set up and data collection procedure described in Section 2.2 was used. Part two involved a faster velocity and the testing facilities water tunnel was not able to produce the increased velocity with a depth more than a few inches. Figure 27 shows the lower water level on the HHA prototype and the test set up is shown below in Figure 33. The data collected for Test 2 can be seen in Figure 31Table 39. All of the same equations that were used for Part 1 Test 1 were used to calculate the variables for Test 2. These variables are shown below in Table 40Table 16 and the calculated power and efficiencies are in Table 41Table 17.

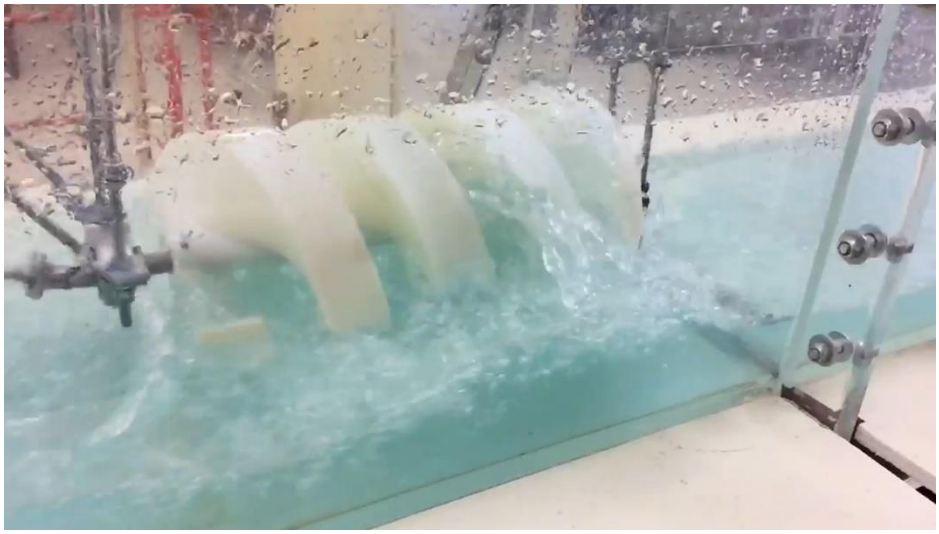

Figure 33: Part 2 Test 3 Experiment Set Up

Table 38: Part 2 Test 3 HHA Design Features

HHA Prototype Design	Pitch (inches)	Blade Revolutions	PVC Pipe Attachment	Edge Feature	Water Velocity (ft/sec)
Auger 4	6	2	N	Y	5.0

Table 39: Part 2 Test 3 Results

Gear Shaft RPM	Generator Shaft RPM	% Area Covered by Water		Average Voltage (volts)	Average Current (amps)	Average Power (watts)
		Front	Back			
145	527	30	40	2.752	0.045	0.125

Table 40: Part 2 Test 3 Power & Efficiency Variables

Variable	Value	Units
Water Density (ρ)	1.940	slugs/ft^3
% Front Area Submerged	30%	-
% Back Area Submerged	40%	-
Average % Area Submerged	35%	-
HHA Length (L_b)	1.0	ft
HHA Outer Radius (R_o)	0.25	ft
HHA Hub Radius (R_i)	0.041	ft
HHA Total Submerged Area (A_b)	0.072	ft^2
HHA Effective Radius (R)	0.072	ft
Coefficient of Drag (C_D)	1.6	-
Relative Velocity (V_r)	3.893	ft/s
Water Velocity (V_C)	5.0	ft/s
Blade Velocity (V_b)	1.107	ft/s
HHA Angular Velocity (ω)	15.184	rad/s
HHA RPM	145	RPM

Table 41: Part 2 Test 3 Power & Efficiency Values

Power & Efficiencies	Value	Units
Force Exerted on HHA Blade (F_D)	1.714	lbf
Potential Power Produced by the HHA (P_T)	1.898	watts
Theoretical Power of the Water Velocity(P_{Th})	14.143	watts
Torque Acting on HHA Shaft (T)	0.125	lbf*ft
Mechanical Power Produced by the HHA (P_M)	1.898	watts
Hydraulic Efficiency of the HHA (η_{hyd})	13.4%	-
Experimental Power Produced by the HHA (P_{Ex})	0.125	watts
Actual Power Efficiency of the HHA (η_A)	7%	-

CHAPTER 4: Results Comparison

4.1 Test Results Summary

All of the test results will be summarized in this section. The HHA prototype descriptions can be referenced from Table 1 and the test parameters for Test 1 and Test 2 can be referenced from Table 2 and Table 3, respectively. A summary of the data for all tests in Part 1 can be found in Table 42 and Table 43. The highest power generated, 0.156 watts, for Part 1 was accomplished in Test 5 using Auger 1.

Table 42: Part 1 Test Results Summary

Test #	HHA Prototype	Pitch (inches)	Shaft RPM	Motor RPM	% Area Covered by Water		Average Voltage (Volts)	Average Current (Amps)	Average Power (Watts)
					Front	Back			
1	Auger 1	4	155	563.64	100	60	2.994	0.049	0.149
2	Auger 2	6	153	556.36	100	60	2.871	0.047	0.137
3	Auger 3	4	135	490.91	100	45	2.506	0.041	0.103
4	Auger 4	6	133	483.64	95	50	2.513	0.041	0.104
5	Auger 1	4	158	574.55	95	45	3.066	0.050	0.156
6	Auger 2	6	155	563.64	85	60	3.001	0.049	0.150

Table 43: Part 1 Efficiencies

Test #	Hydraulic Efficiency	Theoretical Power of the Water Velocity	Experimental Power Produced	Potential Power Produced	Actual Power Efficiency
1	4%	11.088	0.149	0.442	34%
2	4.30%	11.088	0.137	0.475	29%
3	10%	9.702	0.104	0.965	11%
4	9.60%	10.049	0.104	0.961	11%
5	6.70%	9.702	0.159	0.645	24%
6	6.30%	10.049	0.150	0.631	24%

A summary of the data for all tests in Part 2 is in Table 44. The highest power generated, 0.385 watts, for Part 2 was done in Test 2 using Auger 2. This test produced the highest power generated for both parts of the experiment.

Table 44: Part 2 Test Results Summary

Test #	HHA Prototype	Pitch (inches)	Shaft RPM	Motor RPM	% Area Covered by Water		Average Voltage (Volts)	Average Current (Amps)	Average Power (Watts)
					Front	Back			
1	Auger 1	4	170	618	40	40	3.303	0.054	0.182
2	Auger 2	6	231	840	30	40	4.759	0.080	0.385
3	Auger 4	6	145	527	30	40	2.752	0.045	0.125

Table 45: Part 2 Efficiencies

Test #	Hydraulic Efficiency	Theoretical Power of the Water Velocity	Experimental Power Produced	Potential Power Produced	Actual Power Efficiency
1	14.70%	16.164	0.182	2.372	8%
2	14.80%	14.143	0.385	2.090	18%
3	13.40%	14.143	0.125	1.898	7%

4.1.1 Motor Efficiency

One variable that is not calculated into the actual power efficiencies of the HHA prototypes is any losses due to motor efficiencies or other efficiencies lost in the mounting bracket design. The motor efficiency losses were not calculated in the actual power efficiencies due to the lack of information supplied for the motor. Other potential losses could have been from the u-joint connections from the main shaft to the drive shaft, the u-joint connection from the drive shaft to the gear shaft, the bearings used on the main shaft. Accurately taking into account those efficiency losses is nearly impossible without the proper documentation. To

attempt an efficiency calculation including additional efficiency losses would require an estimated overall efficiency of the mounting bracket components and the motor.

Using an estimated overall efficiency of 75% for the motor and mounting bracket components the actual power efficiency can be calculated for Part 2 Test 2. Applying the 75% efficiency to, P_T, the Potential Power Produced by the prototype is

$$P_T = 2.090\ watts * 75\%\ efficiency = 1.568\ watts.$$

The potential power produced by the prototype is reduced to 1.568 watts due to the estimated efficiency losses of the motor, u-joint connections, and bearings. Applying this potential power produced to the Actual Power Efficiency Eq. 20 to find the estimated efficiency including losses is

$$\eta_A = \frac{P_{Ex}}{P_T} = \frac{0.385}{1.568} = 25\%.$$

This efficiency calculation including losses increases the prototype efficiency by 7% compared to the actual power efficiency at 18% for Part 2 Test 2. Using this estimate could improve all of the test actual power efficiencies, but without the proper information on the motor unit used in this experiment, an efficiency rating cannot be confidently incorporated into all of the efficiency calculations.

4.2 Design Feature Comparisons

The tests performed were planned so evaluations could be made for each of the HHA prototype designs individually and as pairs. The pitch differences, PVC pipe feature, edge feature, and water velocity were the design features analyzed to determine the best design for the HHA prototypes tested.

4.2.1 Pitch Geometry

The first design feature that was compared was the different pitches between HHA prototypes, the PVC feature was not incorporated into this analysis. Initially, the prediction for this experiment was to see a direct relationship between power generation and HHA pitch design. Figure 34 shows the minimal differences between the two pitches, 4 inches and 6 inches, for the water velocity of 3.5ft/s. Both HHA designs 1 and 2 were successful in generating nearly the same amount of power for this test. HHA designs 3 and 4 power generation was lower than designs 1 and 2, but they had similar power generation to each other even though they had different pitch dimensions. The HHA prototypes 3 and 4 with the edge feature did not perform as well as the designs without the edge feature. This occurred mainly because of the weight of the prototypes. The edge feature added approximately 9 ounces of material weight to Auger 3 and 4. Auger 1 and 2 weighed a little over a half a pound less which required less torque to turn. This data draws the conclusion of pitch differences not being significant at 3.5ft/s water velocity with the prototypes nearly submerged completely. It is possible if the edge feature could have been added without the significant weight, they could have an improved performance.

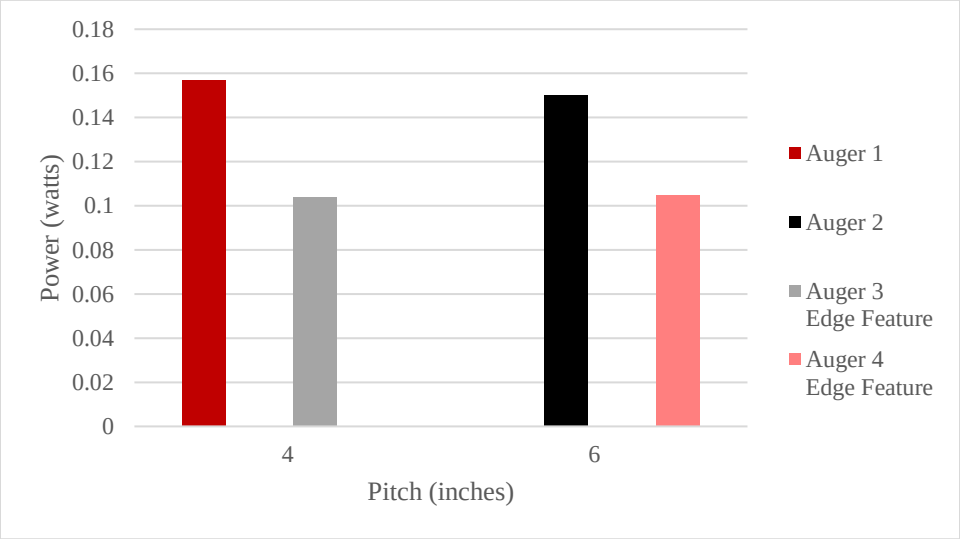

Figure 34: 4" Pitch vs 6" Pitch Power Generation at 3.5ft/s

However, the test data shown in Figure 35 shows a significant difference in power generation at a higher water velocity of 5ft/s and lower water level. The HHA prototype with a pitch of 6 inches generated approximately twice as much power than the HHA prototype with a 4-inch pitch. This data comparison provides a conclusion that HHA power generation is dependent on pitch geometry at water velocities of 5ft/s.

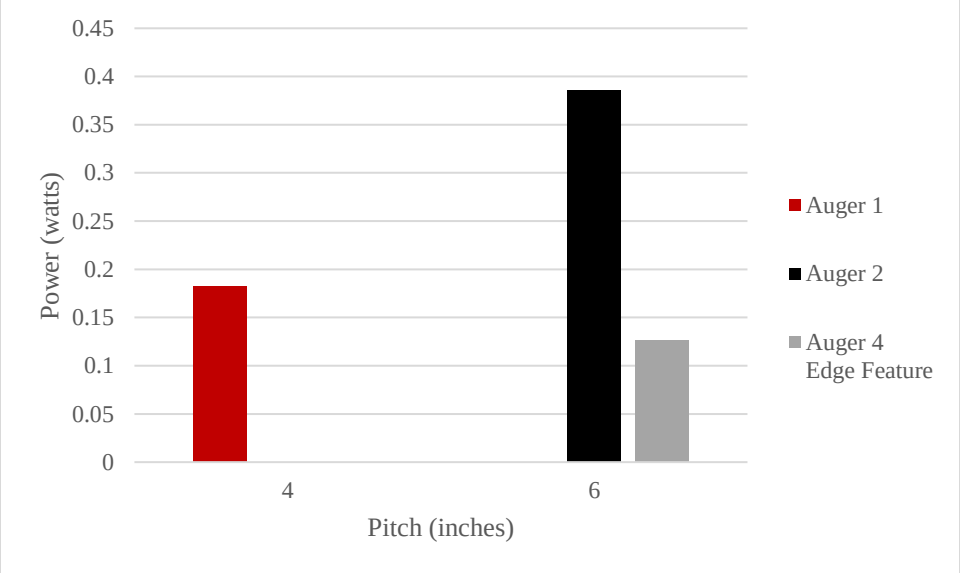

Figure 35: 4" Pitch vs 6" Pitch Power Generation at 5 ft/s

4.2.2 PVC Pipe Feature

The second variable examined in this experiment was the addition of a PVC pipe fitting around the HHA prototype which acted as a duct that funneled the water directly to the auger. The prediction for this feature was increased power generation, conversely, the data displayed opposite results. Figure 36 shows the relationship between the PVC feature addition to the power generated. The PVC feature did not increase power generation for either pitch. From this data, a conclusion that power generation does not increase with the PVC attachment can be made.

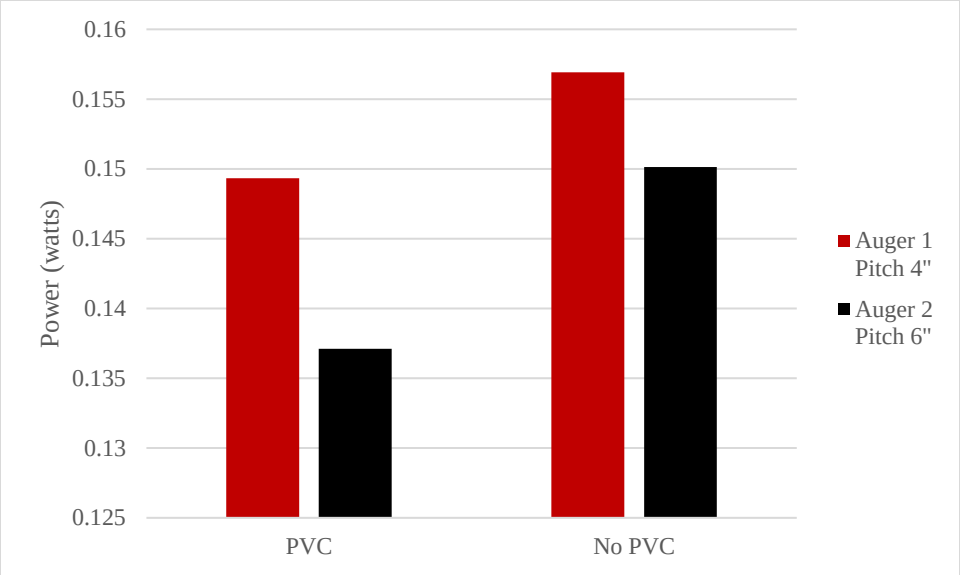

Figure 36: PVC vs No PVC Power Generation at 3.5 ft/s

4.2.3 Edge Feature

The third modification explored for this experiment was the edge feature added to the blade. The idea behind this feature was to simulate a bucket on the edge of the blade that captured the water in the auger instead of allowing the water to escape out the sides of the auger. This design was inspired by the previously discussed Eco-Auger. (3) The prediction for this added feature was that it would produce more power than the plain blade on the HHA prototypes. Figure 37 displays the data comparing the HHA prototypes with and without the edge feature and, as shown below, the prediction for increased power generation was incorrect. The edge feature did not generate more power than the plain blade design. Figure 38 shows data comparing edge feature to plain blades at the increased water velocity of 5ft/s and the same conclusion can be made, the power generation does not increase with the addition of the edge feature.

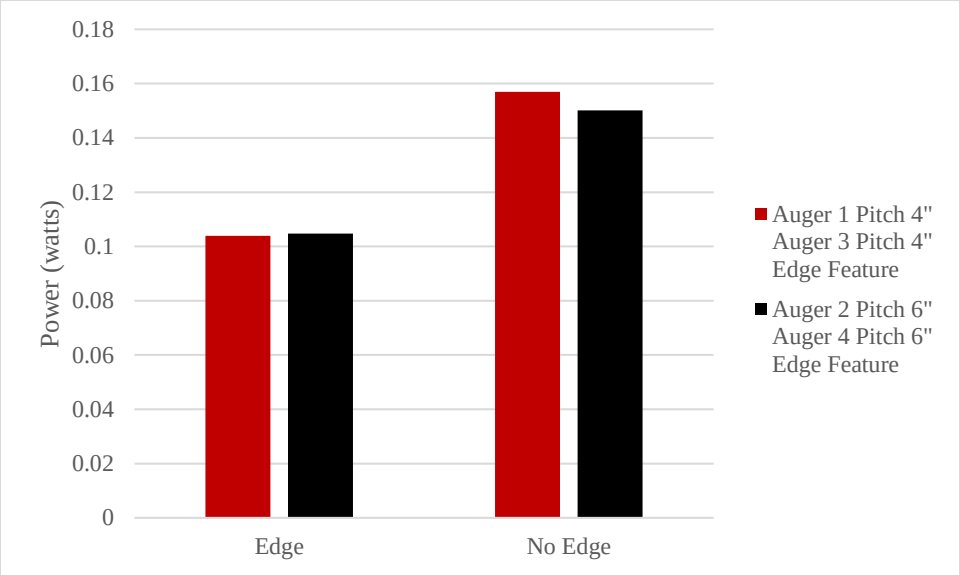

Figure 37: Edge vs No Edge Power Generation at 3.5ft/s

Just as in Chapter 4.2.1, the pitch design in combination with the edge feature did not have a benefit on any design for the slower water velocity, shown in Figure 38Figure 37, but the power generated increased substantially in the faster velocity, shown in Figure 38. This test produced the most power generated out of all of the experiment combinations utilizing HHA prototype 2.

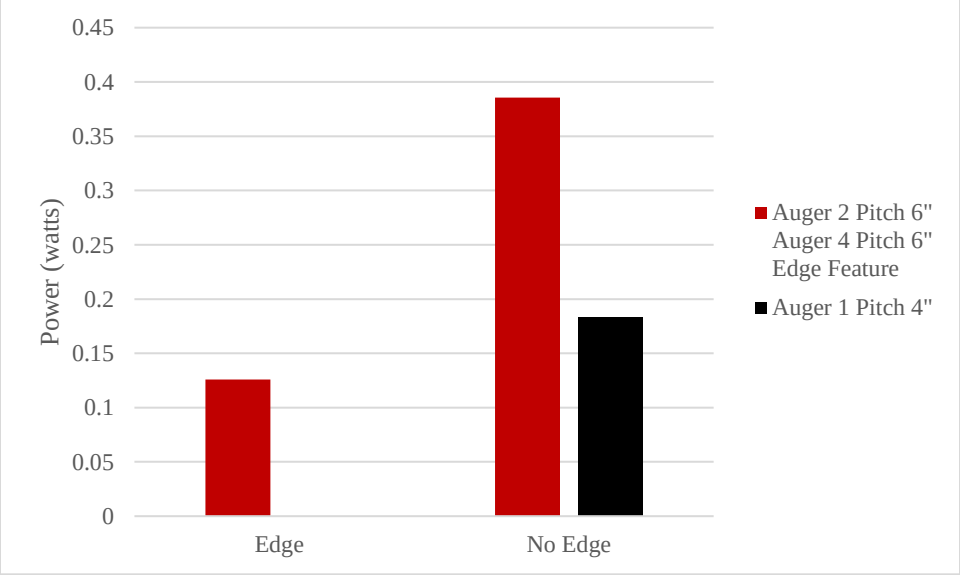

Figure 38: Edge vs No Edge Power Generation at 5ft/s

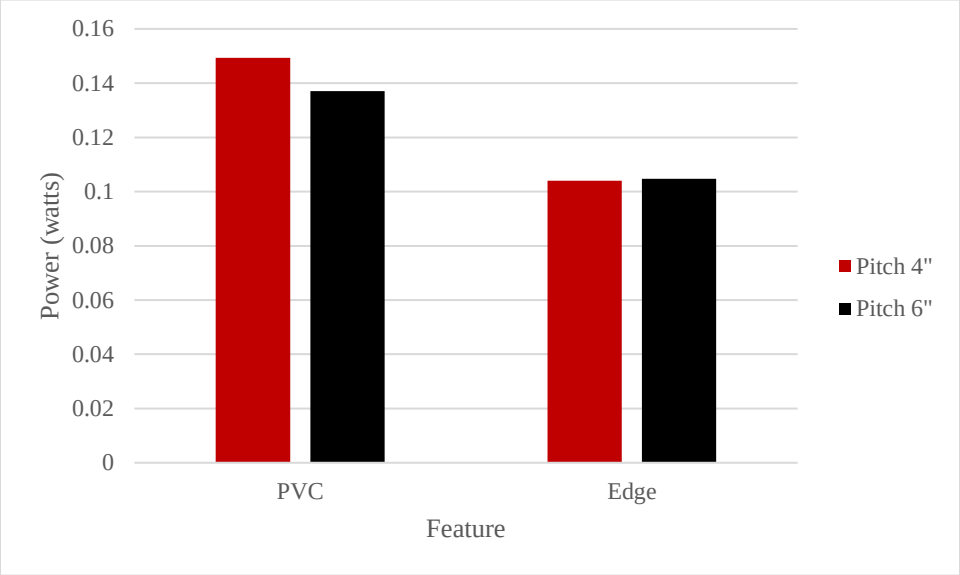

Figure 39: PVC vs Edge Feature Power Generation at 3.5ft/s

The last analysis in this section is relating the PVC feature to the edge feature. The PVC feature allowed for more generated power compared to the edge feature as shown in Figure 39. This data proves that the edge feature was not successful in comparison to the PVC pipe feature.

4.2.4 Water Velocity

The final experiment variable investigated was the two different water velocities and depths. Initially, the test parameters required the HHA prototype to be completely submerged, but with the testing facilities capability this was not accomplished at both velocities. The water velocities tested were 3.5ft/s, with a water depth approximately covering all of the HHA prototype front face, and 5ft/s with a shallower water depth approximately covering a third of the HHA prototype front face. The prediction was the mostly submerged HHA prototypes at 3.5ft/s would generate more power than the HHA prototypes that were only a third submerged at 5ft/s. A comparison of the results for both water velocities tested is shown below in Figure 40.

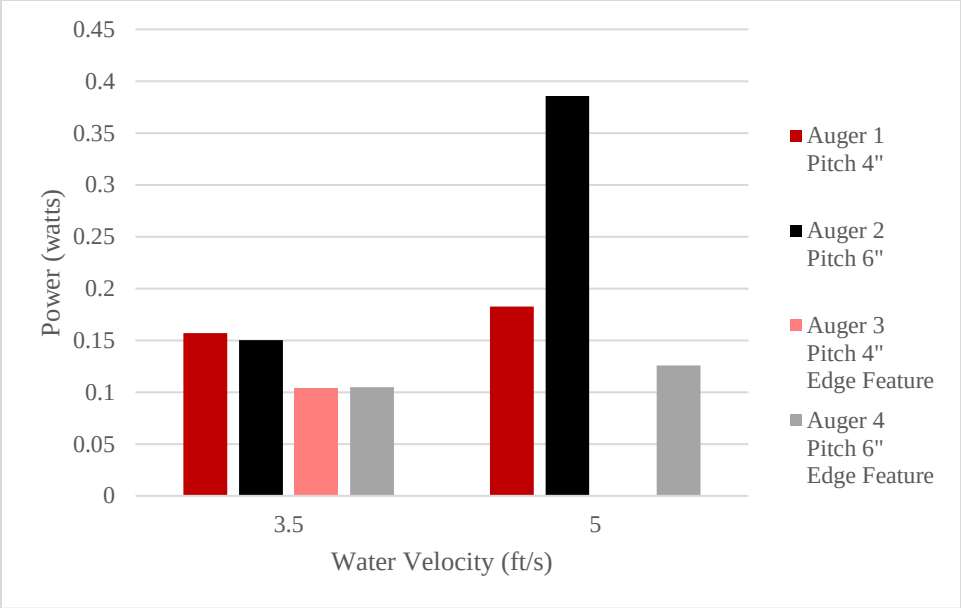

Figure 40: Power Generated vs Water Velocity

Some common themes of the entire experiment such as, the smaller amount of power generated by the designs with the edge feature and the inconclusive pitch and power relationship, are represented in Figure 40. The HHA prototypes generated power at different levels with the change in water velocity. Overall, all three HHA prototypes tested produced more power at 5ft/s than at 3.5ft/s and the HHA designs without the edge feature performed better than the design tested with the edge. Similar to the pitch comparison shown in Figure 35, HHA design 2, with a pitch of 6 inches, generated more power than HHA design 1, which had a pitch of 4 inches at 5ft/s. Figure 40 counters the initial prediction and shows that the faster water velocity, even though it was at a shallower depth, allows the HHA prototypes to generate more power.

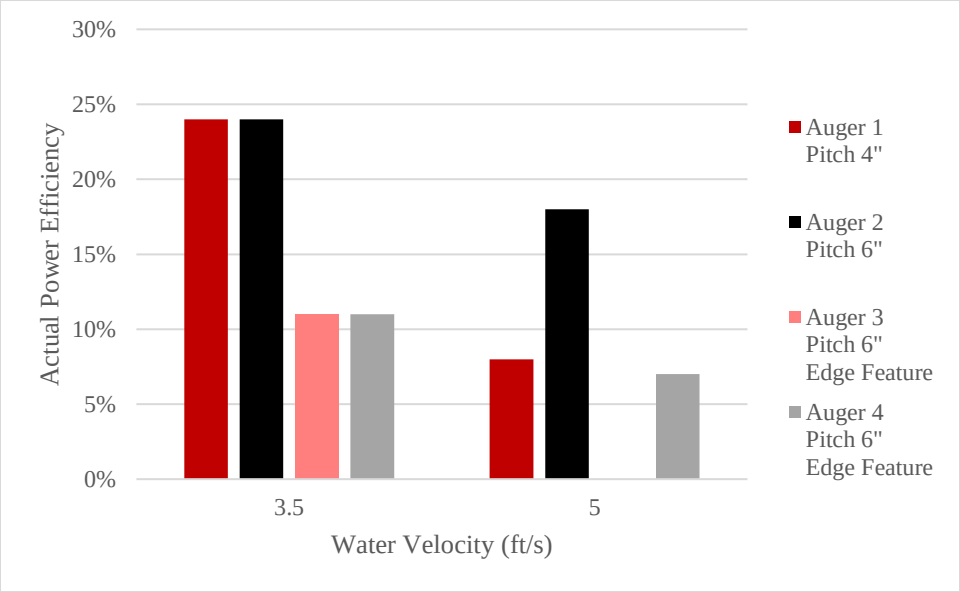

Figure 41: Actual Power Efficiency vs Water Velocity

The theory from Chapter 1.2.3 discussed two different efficiencies, one relating to the theoretical power generation capabilities of the water velocity and the second, the theoretical power generation of the HHA prototype compared to the experimental results which equates to the actual power efficiency of the HHA prototypes. Figure 41 displays the actual power efficiency, the second efficiency calculation, compared to the two different water velocities. The data displayed on Figure 41 indicates the 3.5ft/s water velocity allowed the HHA prototypes to produce power more efficiently, even though it was at a slower velocity. This comparison leads to the conclusion that with a deeper water level and slower velocity, the efficiency of the HHA prototypes will be higher than a shallow water level at a faster velocity.

CHAPTER 5: Summary and Conclusions

5.1 Summary

The goal of this thesis was to design four HHA prototypes, develop a repeatable experimental process to test the power generation capabilities of those prototypes, and provide a recommendation for future work to create an efficient and functional device to harness the kinetic energy of rivers, currents, and other moving bodies of water. The background of the Archimedean screw was discussed in detail along with current screw theory developments in power generation. Examples of potential applications of the Archimedean screw were explored and developed into different horizontal applications. The theory for the potential horizontal applications was discussed in depth.

The designs for each prototype and mounting bracket assembly were described with dimensions and pictures of each item in with different views. The prototypes were fabricated using a 3D printer and the mounting bracket assembly was hand made with various building materials. The HHA mounting bracket and entire test set up was shown in schematics along with all the instruments used in data collection. Each test was explained with a breakdown of figures, data collected, and calculated power and efficiencies. The HHA theory for power generation was utilized for theoretical power and efficiency calculations. The data was separated into four sections: pitch differences, edge feature, PVC feature, and the two different water velocities. These sections were compared and conclusions for the designs and features were made.

5.2 Conclusion

This experiment was successful in testing all of the HHA prototypes, measuring data, and analyzing the data using the reviewed theory. According to the data collected, several conclusions can be made about the experiment findings. The first being that the effectiveness of the pitch dimension is dependent on the water velocity. The HHA prototypes with different pitch dimensions were tested at 3.5ft/s with results being nearly identical. Only when the water velocity was increased a difference in performance was seen. HHA prototype 2 was the most successful with power generation with a pitch of 6 inches in a water velocity of 5ft/s. The conclusion that power generation is not dependent on pitch geometry when the water velocity is 3.5ft/s but, it is dependent when the water velocity is faster at 5ft/s.

The second conclusion made is regarding the tests completed with the PVC feature. In an attempt to potentially generate more power, the PVC pipe feature was added to HHA prototypes 1 and 2. Contradictory to the initial prediction, the power generated by the screw was less with the PVC pipe feature than without it. This feature was only tested at 3.5ft/s and the results conclude that the PVC pipe had a negative effect on the power generation.

The edge feature was the third variable tested and resulted in the third conclusion for this experiment. The bucket like feature added to the edges of the blade was designed to collect water and hold the water in the auger during motion. This was in effort to hold the energy from the water for the entire length of the auger instead of splashing out of the blades in the traditional screw-like design. The testing facilities equipment did not supply a fast enough water velocity with enough depth to be able to fully capture the water in the edge feature as intended or to turn the heavier prototypes fast enough to generate a comparable amount of power to HHA design 2.

The HHA prototypes with the edge feature did not perform as well as the designs without the edge feature.

The last part of the experiment was the change from the 3.5ft/s to 5ft/s water velocity. When the water velocity was increased, the depth of the stream decreased to about a third of the 3.5ft/s water velocity due to the facilities pump capabilities. Three of the HHA prototype designs were tested and HHA design 2 generated the most power out of all the other designs and tests. The increase in power generation was due to the increased water velocity and the pitch of 6-inches. Unlike in the Part 1 of this experiment, the pitch dimension did effect the power generation with the 5ft/s water velocity and HHA design 2 substantially outperformed HHA design 1. Even though the water depth was shallower than Part 1, the HHA prototypes rotated faster and produced more power. However, the actual power efficiency of the HHA prototypes was higher at 3.5ft/s then at 5ft/s. The theoretical values from the calculations for actual power of the HHA was closer to the actual power produced for Part 1. Overall, the conclusion that can be made from Part 2 of the experiment is that with the faster velocity at 5ft/s, more power was generated compared to Part 1.

HHA design 2 performed the best and generated the most power at 5ft/s of any HHA design at either water velocity. According to the efficiency calculations, HHA design 2 was equally as efficient as HHA design 1 at 3.5ft/s and 10% more efficient at 5ft/s than HHA design 1. The recommended prototype design would be HHA design 2 based on the experimental findings described in this thesis.

5.3 Future Work

The recommended design, HHA design 2, could be used to influence the development of similar horizontal Archimedean screw applications. This design should be investigated and tested

in depth with an applicable water tunnel to simulate a fully submerged state at similar and faster velocities. In addition to controlled environment testing, additional tests should be performed in actual bodies of water to understand the potential of actual power generation in a fluctuating real life setting. The actual efficiencies of HHA design 2 should be investigated along with motor and mounting bracket efficiencies. One design feature that should be modified is the edge feature. This feature should be redesigned to create a lighter weight prototype and tests should be redone in both velocities.

REFERENCES

1. *Simplified Theory of Archimedean Screws.* Muller, Gerald and Senior, James. 5, 2009, Journal of Hydraulic Research, Vol. 47, pp. 666-669.

2. *Investigating the Hyrdodynamic Behavior of Innovative Archimedean Hydropower Turbines.* Stergiopoulou, Alkistis and Kalkani, Efrosini. 1, 2013, International Journal of Recent Research and Applied Studies, Vol. 17, pp. 87-96.

3. eco-auger international inc. [Online] http://eco-auger.com/.

4. *Towards an Innovative Radial Flow Impulse Turbine and a New Horizontal Archimedean Hydropower Screw.* Mayrhofer, Bernhard, et al. 2, 2014, Journal of Energy and Power Sources, Vol. 1, pp. 72-78.

5. Munson, Bruce R, et al. *Fundamentals of Fluid Mechanics.* 7. Hoboken : John Wiley & Sons, 2013. pp. 513-529.

6. PolyJet Material Selection Guide. *Stratasys.* [Online] http://www.stratasys.com/materials/polyjet/rigid-opaque.

7. PolyJet Technology. *Stratasys.* [Online] http://www.stratasys.com/3d-printers/technologies/polyjet-technology.

8. *The Turn of the Screw: Optimal Design of an Archimedes Screw.* Rorres, Chris. 2000, Journal of Hyrdaulic Engineering, pp. 72-80.

9. *Modeling of Archimedes Turbine for Low Head Hyrdo Power Plant in Simulink MATLAB.* Raza, Ali, Mian, Muhammad Saleem and Saleem, Yasir. 7, 2013, International Journal of Engineering Research & Technology , Vol. 2, pp. 2471-2477.